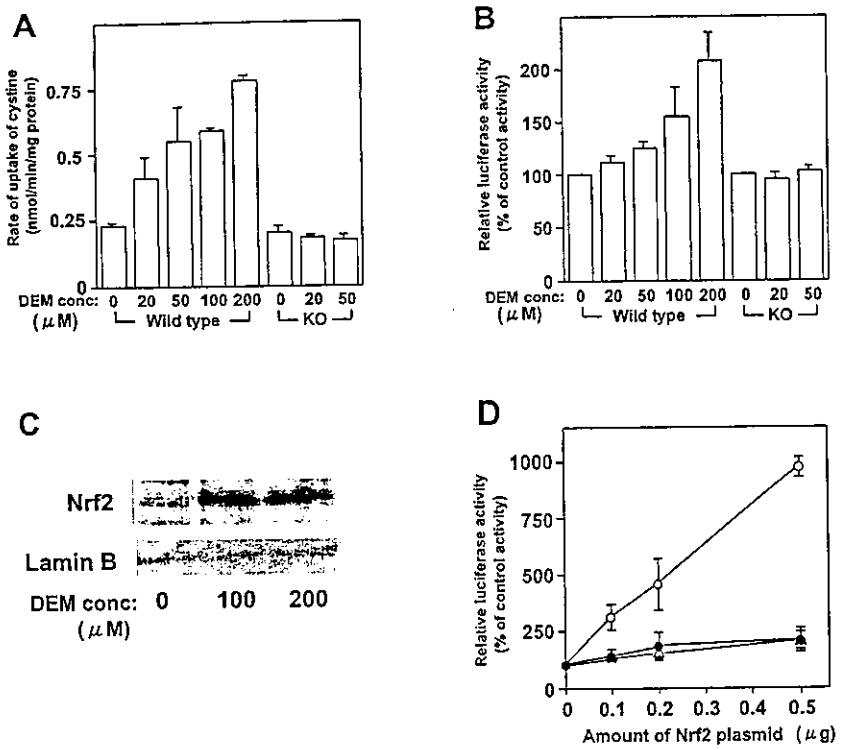

FIG. 10. **Involvement of Nrf2 in the transcriptional regulation of xCT gene.** *A*, mouse embryonic fibroblasts derived from wild type mice (*Wild type*) and Nrf2-deficient mice (*KO*) were incubated for 24 h after plating, and the cells were further incubated for 12 h with DEM at the concentrations indicated. Then, the activity of cystine transport was measured. *B*, the cells were incubated for 24 h after plating, transfected with pGL3–0.23, and further incubated for 24 h. Then, the cells were incubated for 12 h with DEM at the concentrations indicated, and luciferase activity was measured. *C*, the embryonic fibroblasts derived from wild type mice were incubated for 24 h after plating and further incubated for 6 h with or without 100–200 μM DEM. The nuclear extract was prepared from the cells, and Western blot analysis was performed using anti-Nrf2 antibody. *D*, the embryonic fibroblasts derived from wild type mice were co-transfected with the Nrf2 expression plasmid of the amount indicated and pGL3–0.08 (●), pGL3–0.12 (△), or pGL3–0.23 (○). After incubating for 24 h, the luciferase activity was measured.

scription is probably EpRE-1. EpRE-2 has two nucleotide mismatches at −120 and −116, compared with the consensus EpRE proposed by Erickson *et al.* (21). The luciferase activities in the cells transfected with the constructs containing the mutations in EpRE-1 were significantly decreased despite the treatment with DEM. In the 5′-flanking region of human xCT gene, EpRE-2 is deficient. It is unlikely that EpRE-2 contributes to DEM-inducible transcription of xCT gene by itself. EpRE-3 completely matches the consensus EpRE proposed by Erickson *et al.* (21), whereas EpRE-4 has two nucleotide mismatches. EpRE-3 is completely conserved in the 5′-flanking region of human xCT gene, whereas EpRE-4 is not completely conserved in the human xCT gene. However, the luciferase activity in the cells transfected with pGL3–0.08, which contains EpRE-3 and -4, was negligible irrespective of the treatment with DEM. Thus, EpRE-3 and -4 by themselves do not contribute to the DEM-inducible transcription of xCT gene. The luciferase activity in the cells transfected with the constructs containing the mutations in EpRE-1 increased slightly but significantly by treatment with DEM. These results suggest that other EpREs, particularly EpRE-3, may contirubute to the enhancement of the DEM-inducible transcription in cooperation with EpRE-1.

Recently, Itoh *et al.* (15) have demonstrated that Keap 1, the cytosolic protein, interacts with Nrf2 to form a complex in the cytosol and that DEM causes the dissociation of the complex and then Nrf2 moves into the nucleus to enhance the EpRE-mediated transcription of the genes in cooperation with small Maf protein. In the present study, Nrf2 has been demonstrated to mediate the induction of the transcriptional activity of xCT gene by DEM via the EpRE. DEM probably plays a role in dissociation of Nrf2-Keap 1 complex, because the overexpression of Nrf2 enhances the transcription of xCT gene even in the absence of DEM (Fig. 10*D*).

In the present study, we have demonstrated that the intracellular cysteine levels are increased in BHK21 cells when they are treated with the stress agents. Most probably this increase is accounted for by the induction of system x_c^- activity as shown previously in other cells (27). The concentration of the cysteine in the cells untreated and treated with DEM can be estimated to be ~0.1 and 0.3 mM, respectively, assuming that 1 mg of cell protein is equivalent to 5 μl of cell water (28). γ-GCS is known to catalyze the rate-limiting step in synthesis of GSH, and its apparent K_m value for cysteine is reported to be 0.35 mM (29). Thus, the rate of GSH synthesis in BHK21 cells treated with DEM is much higher than that in the control cells even if γ-GCS *per se* remains unchanged. Mulcahy *et al.* (22, 23) have demonstrated that the EpREs in the 5′-flanking regions of the genes encoding γ-GCS heavy and light subunits regulate the expression of these genes in the cells treated with β-naphtoflavone, an electrophilic agent, which induces phase II enzymes. In the cells treated with DEM, both the increase in intracellular cysteine levels caused by the induction of the activity of system x_c^- and the induction of γ-GCS seem to contribute to the increase in GSH synthesis.

REFERENCES

1. Bannai, S., and Kitamura, E. (1980) *J. Biol. Chem.* **255**, 2372–2376
2. Watanabe, H., and Bannai, S. (1987) *J. Exp. Med.* **165**, 628–640
3. Cho, Y., and Bannai, S. (1990) *J. Neurochem.* **55**, 2091–2097
4. Bannai, S., and Tateishi, N. (1986) *J. Membr. Biol.* **89**, 1–8
5. Bannai, S., Sato, H., Ishii, T., and Sugita, Y. (1991) *Biochim. Biophys. Acta* **1092**, 175–179
6. Sato, H., Fujiwara, K., Sagara, J., and Bannai, S. (1995) *Biochem. J.* **310**, 547–551
7. Sato, H., Tamba, M., Ishii, T., and Bannai, S. (1999) *J. Biol. Chem.* **274**, 11455–11458
8. Verrey, F., Meier, C., Rossier, G., and Kühn, L. C. (2000) *Pflügers Arch. Eur. J. Physiol.* **440**, 503–512
9. Rushmore, T. H., King, R. G., Paulson, K. E., and Pickett, C. R. (1990) *Proc. Natl. Acad. Sci. U. S. A.* **87**, 3826–3830
10. Friling, R. S., Bensimon, A., Tichauer, Y., and Daniel., V. (1990) *Proc. Natl. Acad. Sci. U. S. A.* **87**, 6258–6262
11. Favreau, L. V., and Pickett, C. B. (1991) *J. Biol. Chem.* **266**, 4556–4561
12. Rushmore, T. H., Morton, M. R., and Pickeet, C. B. (1991) *J. Biol. Chem.* **266**, 11632–11639
13. Wasserman, W. W., and Fahl, W. E. (1997) *Proc. Natl. Acad. Sci. U. S. A.* **94**, 5361–5366
14. Itoh, K., Chiba, T., Takahashi, S., Ishii, T., Igarashi, K., Katoh, Y., Oyake, T., Hayashi, N., Satoh, K., Hatayama, I., Yamamoto, M., and Nabeshima, Y. (1997) *Biochem. Biophys. Res. Commun.* **236**, 313–322
15. Itoh, K., Wakabayashi, N., Katoh, Y., Ishii, T., Igarashi, K., Engel, J. D., and Yamamoto, M. (1999) *Gene Dev.* **13**, 76–86
16. Ishii, T., Itoh, K., Takahashi, S., Sato, H., Yanagawa, T., Katoh, Y., Bannai, S., and Yamamoto, M. (2000) *J. Biol. Chem.* **275**, 16023–16029

17. Tiemann, F., and Deppert, W. (1994) *Oncogene* **9,** 1907–1915
18. Cotgreave, I. A., and Moldéus, P. (1986) *J. Biochem. Biophys. Methods* **13,** 231–249
19. Sagara, J., Miura, K., and Bannai, S. (1993) *J. Neurochem.* **61,** 1667–1671
20. Tietze, F. (1969) *Anal. Biochem.* **27,** 502–522
21. Erickson, A. M., Nevarea, Z., Gipp, J. J., and Mulcahy, R. T. (2002) *J. Biol. Chem.* **277,** 30730–30737
22. Mulcahy, R. T., Wartman, M. A., Bailey, H. H., and Gipp, J. J. (1997) *J. Biol. Chem.* **272,** 7445–7454
23. Moinova, H. R., and Mulcahy, R. T. (1998) *J. Biol. Chem.* **273,** 14683–14689
24. Campagne, M. L., Thibodeaux, H., Bruggen, N., Cairns, B., and Lowe, D. G. (2000) *J. Neurosci.* **20,** 5200–5207
25. Kim, Y. C., Masutani, H., Yamaguchi, Y., Itoh, K., Yamamoto, M., and Yodoi, J. (2001) *J. Biol. Chem.* **276,** 18399–18406
26. Sato, H., Tamba, M., Kuriyama-Matsumura, Okuno, S., and Bannai, S. (2000) *Antioxid. Redox Signaling* **2,** 665–671
27. Bannai, S., and Ishii, T. (1982) *J. Cell. Physiol.* **112,** 265–272
28. Sato, H., Watanabe, H., Ishii, T., and Bannai, S. (1987) *J. Biol. Chem.* **262,** 13015–13019
29. Richman, P. G., and Meister, A. (1975) *J. Biol. Chem.* **250,** 1422–1426
30. Sato, H., Kuriyama-Matsumura, K., Hashimoto, T., Sasaki, H., Wang, H., Ishii, T., Mann, G., and Bannai, S. (2001) *J. Biol. Chem.* **276,** 10407–10412

tapraid4/h7-phys/h7-phys/h70303/h70267d03a | moyerr | S=11 | 9/18/02 | 22:07 | MS: PG0112-1 | Int: 11e/mg\ejp

Physiol Genomics 11: 000–000, 2002.
First published August 27, 2002; 10.1152/physiolgenomics.00112.2001.

Isolation and characterization of zebrafish NFE2

STEPHEN J. PRATT,[1,2,*] ANNA DREJER,[2,*] HELEN FOOTT,[1,2,*]
BRUCE BARUT,[1,2] ALISON BROWNLIE,[1,2] JOHN POSTLETHWAIT,[5]
YASUTAKE KATO,[6] MASAYUKI YAMAMOTO,[6] AND LEONARD I. ZON[1,2]
[1]*Howard Hughes Medical Institute,* [2]*Children's Hospital, Division of Hematology/Oncology,*
[3]*Dana-Farber Cancer Institute, and* [4]*Harvard Medical School, Boston, Massachusetts 02115;*
[5]*Institute of Neuroscience, University of Oregon, Eugene, Oregon 97403; and* [6]*Center for TARA,*
AQ: 1 *University of Tsukuba, 1-1-1 Tennoudai, Tsukuba 305-8577, Japan*

Received 3 December 2001; accepted in final form 9 August 2002

Pratt, Stephen J., Anna Drejer, Helen Foott, Bruce Barut, Alison Brownlie, John Postlethwait, Yasutake Kato, Masayuki Yamamoto, and Leonard I. Zon. Isolation and characterization of zebrafish NFE2. *Physiol Genomics* 11: 000–000, 2002. First published August 27, 2002; 10.1152/physiolgenomics.00112.2001.—Vertebrate hematopoiesis is regulated by distinct cell-specific transcription factors such as GATA-1 and SCL. Mammalian p45-NFE2 was characterized for its ability to bind the hypersensitive sites of the globin locus control region. NFE2 is a member of a cap'n'collar (CNC) and basic zipper (BZIP) superfamily that regulates gene transcription. It has been implicated in diverse processes such as globin gene expression, oxidative stress, and platelet lineage differentiation. Here, we have isolated the zebrafish ortholog of NFE2. The gene is highly homologous, particularly in the DNA-binding domain. Mapping the zebrafish NFE2 to linkage group 23 establishes a region of chromosomal synteny with human chromosome 12, further suggesting evolutionary conservation. During embryogenesis, the zebrafish gene is expressed specifically in erythroid cells and also in the developing ear. NFE2 expression is lacking in zebrafish mutants that have no hematopoietic cells. An analysis of the *sauternes* mutant, which carries a mutation in the ALAS-2 gene and thus has defective heme synthesis, demonstrates higher levels of NFE2 expression than normal. This further establishes the block to erythroid differentiation in the *sauternes* mutant. Our studies demonstrate conservation of the vertebrate genetic program for the erythroid lineage.

hematopoiesis; transcription factors; erythroid lineage; *sauAQ: 3 ternes* mutant

HEMATOPOIESIS involves the production of hematopoietic stem cells, with subsequent cell proliferation and differentiation. This process is regulated by transcription factors specifically expressed in hematopoietic cells (5). AQ: 4 The erythroid program has been extensively characterized in vertebrate species, and the transcription factors GATA-1 and GATA-2 directly activate promoters and enhancers of many, if not all, erythroid genes. The factors SCL and LMO2 have recently been shown to regulate the earliest stage of the hematopoiesis. The recent finding of a cofactor of GATA-1, called FOG1, also demonstrates the regulation of transcription by complexes of proteins (45).

The factor p45-NFE2 is a member of the basic zipper (BZIP) transcription factor family and contains a cap'n'collar (CNC) motif (2, 3). p45-NFE2 was originally isolated due to its ability to bind a duplicated AP-1 site TGCTGA(G/C)TCA(T/C) in the hypersensitive site 2 (HS2) region of the globin locus control region (43). This factor was subsequently shown to heterodimerize with members of the maf family of transcription factors, which also encode BZIP proteins (4, 18). p45-NFE2 is a member of a family of factors that are also known as NRF1, NRF2, and NRF3 (7, 9, 11, 22). NRF1 and NRF2 are also known as LCRF1 and LCRF2. Bach1 and Bach2 are also new members of this family. These factors are able to bind similar sites of the globin HS2 locus (34). p45-NFE2 has been targeted by homologous recombination in mouse embryonic stem cells, and the mouse knockout demonstrates that the factor is critically required for platelet production (23, 24). Consistent with this, a hematopoietic-specific tubulin has been shown to be a target of p45-NFE2 (23). The NFE2 −/− animals also have a mild microcytic anemia, suggesting p45-NFE2 does have a role in hemoglobin production (39). Further support for a role of this transcription factor in erythropoiesis comes from in vitro studies. An erythroid cell line deficient in p45-NFE2 fails to differentiate (25), whereas ectopic expression of NFE2 in a myeloid cell line induces erythroid differentiation (38). NRF1 and NRF2 have each been inactivated in mouse embryonic stem cells, and it is apparent that these factors do not participate in erythropoiesis in a cell autonomous manner (10, 11, 15, 28).

The zebrafish is a new developmental and genetic system for studying organ development and embryogenesis (17) and is well suited for the analysis of hematopoiesis. Several forward genetic screens have identified mutants with defective erythropoiesis (1). To date there are 26 complementation groups of hematopoietic mutants, each with defects in distinct stages of

Article published online before print. See web site for date of publication (http://physiolgenomics.physiology.org).

Address for reprint requests and other correspondence: L. I. Zon, Howard Hughes Medical Institute, Children's Hospital, Enders 7, 300 Longwood Ave., Boston, MA 02115 (E-mail: zon@enders.tch.harvard.edu).
*S. J. Pratt, A. Drejer, and H. Foott contributed equally to this work.

development (36, 46). There are mutants that effect dorsal-ventral patterning, hemangioblast formation, hematopoietic stem cell production, proliferation, and differentiation. In addition, there are several mutants with defects in the production of hemoglobin or with defects in heme biosynthesis. The cloning of the genes for some of these mutants has demonstrated the conservation of the hematopoietic program. For instance, the *sauternes* gene encodes ALAS-2 (6). The *sauternes* mutant has hypochromic anemia and is reminiscent of the human ALAS-2 deficiency syndrome, congenital sideroblastic anemia. A mutation in β-spectrin in the *riesling* mutant leads to hereditary spherocytosis (27). Novel genes have also been obtained in this zebrafish system. We recently isolated a novel iron exporter, called ferroportin-1, that regulates the transport of iron from the yolk to the embryonic circulation (14).

We have begun to define the hematopoietic program in the zebrafish by isolating transcription factors known to regulate hematopoiesis in higher vertebrates. To date, we have isolated the genes encoding GATA-1, -2, and -3, SCL, LMO2, *fli1*, and c-*myb* (12, 44). In an effort to further characterize the program, we sought to isolate the NFE2 transcription factor in zebrafish. NFE2 is expressed in an erythroid-specific manner, and its expression is not detected in *cloche*, a zebrafish mutant with defective hematopoiesis (41). Gel mobility shift analysis demonstrated that zebrafish and mammalian NFE2 can bind similar sequences. CNC-BZIP factors are located near Hox clusters in mammals (22, 26). Mapping of zebrafish NFE2 near the HoxC cluster of LG23 demonstrated conservation of synteny with humans, suggesting that NFE2 function is also conserved throughout vertebrate evolution.

METHODS

Isolation of cDNA clone for zebrafish NFE2. A PCR fragment of 180 bp encoding the DNA-binding domain of mouse p45-NFE2 (a gift from Nancy Andrews) was used to screen a gridded adult zebrafish kidney cDNA library (Research Genetics, and RZPD). The library consisted of 92,160 oligo dT primed clones and 92,160 random primed clones in the pBK-CMV cloning vector (Stratagene). The mouse p45-NFE2 fragment was randomly primed with [^{32}P]dCTP for 2 h and hybridized to the filters at 55°C overnight. The filters were then washed to 0.2× SSC at 55°C and exposed to autoradiography film overnight. Hybridizing clones were then sequenced to determine their identity.

In situ hybridization. In situ hybridization was performed as described (44). Antisense riboprobes for the zebrafish NFE2 were made by digesting the cDNA with the restriction enzyme *Eco*RI and utilizing T7 RNA polymerase as described (44).

Genotyping of sauternes mutants. Sauternes embryos stained for NFE2 expression were photographed before extracting DNA. Scored embryos were then genotyped using the previously described markers E9.T3F5/R3 (F5, 5′-CACCAAATGAATTGGATTTG-3′; R3, 5′-AAAACAAACAGATCCCATTC-3′). Fifteen fish with increased NFE2 expression were genotyped as mutant with one mis-score.

Mapping of zebrafish NFE2. A single bacterial artificial chromosome (BAC) clone was obtained by hybridizing the zebrafish p45-NFE2 complete cDNA to BAC filters (Genome Systems). The cDNA was randomly primed with [^{32}P]dCTP for 2 h and hybridized to the filters at 65°C overnight. The filters were then washed to 0.1× SSC at 65°C and exposed to autoradiography film overnight. The ends of the BAC were directly sequenced and primers (NFE2BACSP6, F1-TCCTATTTCACCAGCCAAGAACTG; and NFE2BACSP6, R1-CAAAAGGAGGTTTCTCAGCGATGC) were designed for single-strand conformational polymorphism (SSCP) analysis. A 200-bp band was generated that segregated in the genetic mapping panels (16, 20).

Other plasmids. The cDNA plasmids encoding either mouse p45-NFE2, zebrafish NF-E2, or mouse MafK were subcloned in pIK111 (18) and pBK-CMV-zp45 and pmMafK15 (30), respectively.

In vitro transcription/translation. One microgram of each of the cDNA constructs encoding mouse p45-NFE2, zebrafish NFE2, or mouse Maf K were transcribed and translated in vitro using the TNT T7 or T3 Coupled Wheat Germ Extract System (Promega).

Gel mobility shift assay. The binding mixture (10 μl) contained 250 pg of the radiolabeled oligonucleotide probe no. 25 (21), 20 mM HEPES-KOH (pH 7.9), 1 mM EDTA, 20 mM KCl, 5 mM DTT, 4 mM $MgCl_2$, 1,000 μg/ml of poly(dI-dC), 100 μg/ml of BSA, and 5 μl of in vitro translated material. The resultant protein-DNA complexes and free probe were electrophoresed

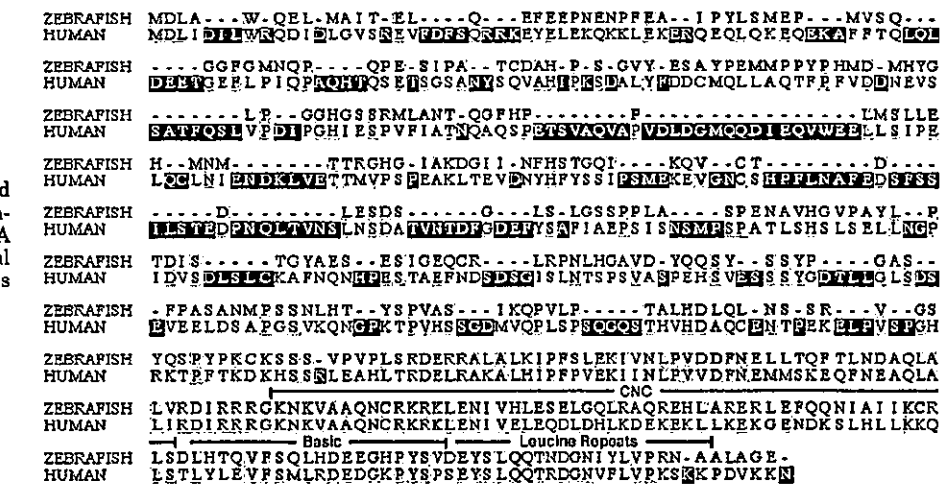

Fig. 1. Comparison of zebrafish and human NFE2 cDNAs. Note the extensive degree of identity in the DNA binding domain in the COOH-terminal region of the sequence. Identity is shaded in gray.

through a 4% polyacrylamide gel in 0.5× TBE buffer at 25°C. A 400-fold molar excess of unlabeled oligonucleotide was added to the reaction as a specific competitor (30).

RESULTS

Isolation of zebrafish NFE2. Utilizing a mouse p45-NFE2 cDNA probe, we screened a gridded zebrafish kidney cDNA library and identified seven hybridizing clones. These clones were isolated and sequenced, and one clone (139 O4) was found to encode a protein related to mammalian p45-NFE2. A comparison of the zebrafish cDNA to human NFE2 revealed that the structure has largely been conserved during vertebrate evolution, particularly in the BZIP and CNC regions

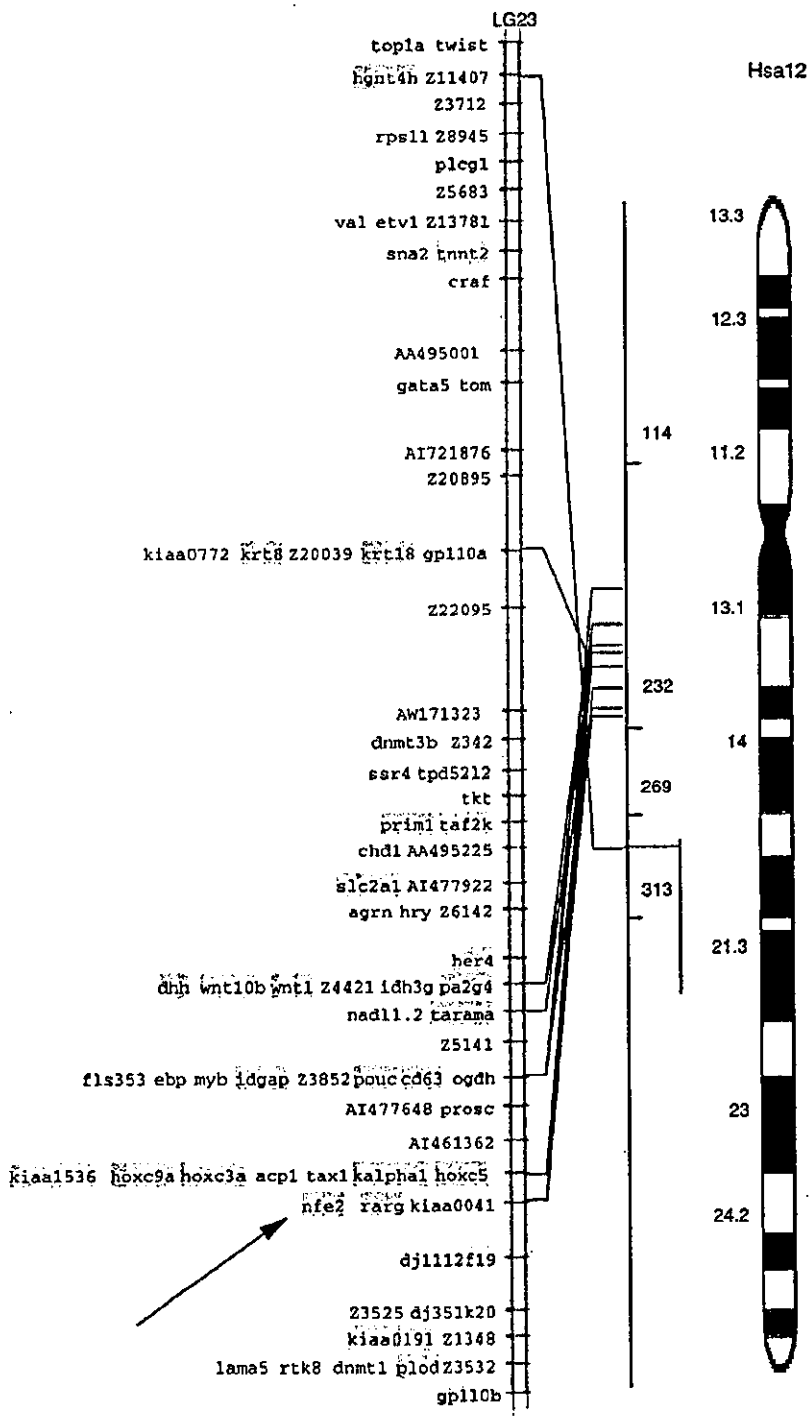

Fig. 2. Chromosomal localization of NFE2 to linkage group 23 and synteny with human chromosome 12.

COLOR

taprai d4/h7-phys/h7-phys/h70303/h70267d03a | moyerr | S=11 | 9/18/02 | 22:10 | MS: PG0112-1 | Inl: 11e/mg\ejp

Table 1. *An analysis of the genetic mapping for NFE2*

Locus	M	P	X	*N*	Map Interval, cM	95% CI, cM	LOD
hoxc5a	42	54					
			1	46	2.17 ± 2.15	0.1 to 11.5	11.8
nfe2	22	24					
			7	46	15.22 ± 5.30	6.3 to 28.9	5.3
z3157	45	51					

Locus, *hoxc5a* (Y14539), *nfe2* (this work), *z3157* (ZFIN ID: ZDB-SSLP-980528-342); M, maternal genotype; P, paternal genotype; X, cross-overs; *N*, number scored; Map Interval, map interval ± SE; 95% CI, 95% confidence interval; LOD, logarithm of the odds score.

F1 (Fig. 1), but the domains outside of the BZIP region are relatively divergent.

Positioning of NFE2 to the zebrafish genome map. To evaluate the map location of the zebrafish NFE2 gene and to determine whether NFE2 was a potential candidate for any of the currently mapped zebrafish hematopoietic mutants, a BAC clone (85 K11) was isolated, and its ends were mapped utilizing both a genetic backcross panel as well as a radiation hybrid panel. It was found that NFE2 mapped to linkage group 23 between RAPD marker 8A.800 and the HoxC F2 T1 cluster (20, 35) (Fig. 2 and Table 1). This map position does not correspond to any of our mutants. Interestingly, the region of LG23 on which NFE2 lies is highly syntenic to human chromosome 12 and mouse chromosome 15 (Fig. 2) (35) where human and mouse NFE2 AQ: 9 map, respectively. The similar structure of the zebrafish cDNA with mammalian NFE2, taken together with the chromosomal synteny, indicates that this gene has been conserved throughout vertebrate evolution.

Analysis of gene expression. Expression pattern of NFE2 during embryonic development was examined by whole embryo in situ hybridization (Fig. 3). NFE2 F3 initiates expression at 10 somites in the developing intermediate cell mass (ICM) in a pattern very similar to that of GATA-1 (12). As development continues from 18 somites to 24 h, the gene is more highly expressed in the developing ICM, the functional equivalent of the mammalian yolk sac. Thus NFE2 appears to be induced during erythroid differentiation rather than being expressed in the early hematopoietic cell population. After 36 h, NFE2 is expressed at a much lower level in circulating blood cells. In addition, we find NFE2 transcripts in the developing otic vesicle.

Analysis of the NFE2 expression in mutant zebrafish. We first analyzed NFE2 expression in the mutant *cloche* (Fig. 4). Expression of GATA-1 is deficient in F4 *cloche* mutants (41), consistent with an absence of blood as previously described. NFE2 expression in the blood forming regions, similarly to GATA-1, is absent in *cloche* (44). This confirms the hematopoietic-specific expression of NFE2. In *cloche* the expression in the developing ear is still present, suggesting that *cloche* is not defective at the NFE2 locus.

We subsequently analyzed the expression of NFE2 in the *sauternes* mutant (ALAS-2 deficiency) (Fig. 5). We F5 have previously demonstrated alterations of gene expression in the *sauternes* mutant (6). GATA-1 expression in wild type embryos is down regulated by *day 3*. However, in *sauternes* mutants, GATA-1 expression is

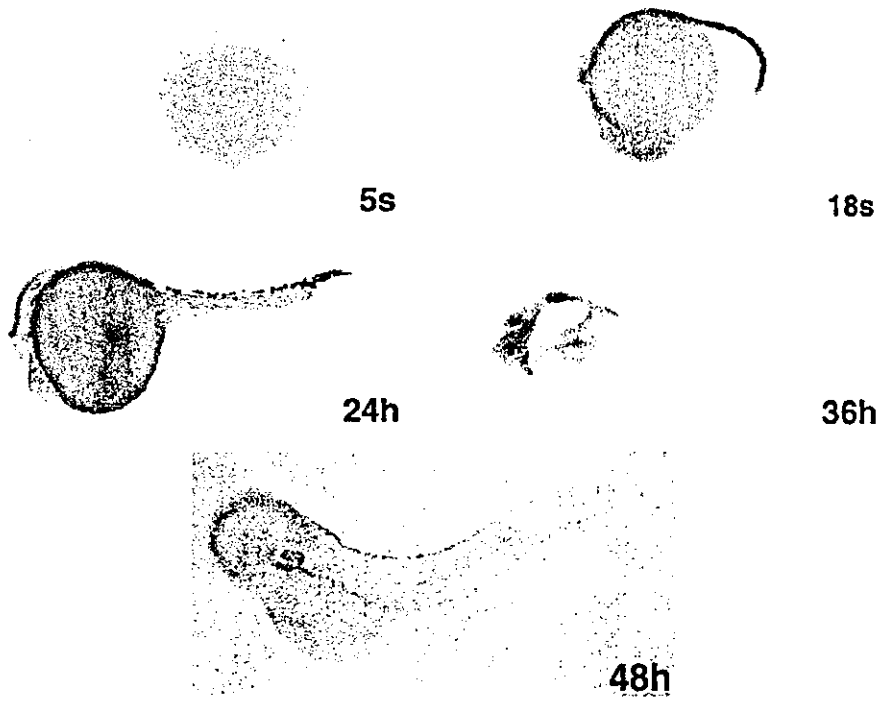

COLOR AQ: 14 Fig. 3. Whole embryo in situ hybridization studies for NFE2 expression during development. The stages are indicated, from 5 s to 48 h.

COLOR

Fig. 4. Analysis of the zebrafish mutant *cloche*. The *cloche* mutant lacks blood and blood vessel cells and has no NFE2 expression in the developing blood island. Expression is detected in the otic vesicle in wild-type (wt) and *cloche* embryos.

not downregulated by *day 3* of development. We find that similar to GATA-1, NFE2 is also not downregulated by *day 3* of development (Fig. 5). The downregulation of GATA-1 and NFE2 suggests the transcription of these genes is regulated by heme levels. This indicates a block to hematopoietic differentiation in the cells in circulation of *sauternes* mutants.

Characterization of zebrafish NFE2 protein. We sought to characterize whether zebrafish NFE2 could bind similar sites as the mammalian protein. Mammalian p45-NFE2 can bind to an NFE2 site in the pres- AQ: 10 ence of mafK (21). Zebrafish NFE2 was expressed in wheat germ extract. In the presence of expressed mafK, a gel mobility shift reminiscent of the mammalian p45-NFE2/mafK heterodimer is seen (Fig. 6, *lane* F6 7), whereas homodimers do not bind. The binding is specific since it was competed with excess unlabeled oligonucleotide. NFE2 sites have yet to be described in zebrafish genes involved in hematopoiesis, although only few genes have been examined. Our studies suggest NFE2 sites will be found in the globin locus and in thrombocyte-specific genes of the zebrafish.

DISCUSSION

The vertebrate hematopoietic program is highly conserved, particularly for the transcription factors involved in hematopoiesis (33). We believe that the zebrafish NFE2 gene is the true ortholog because the zebrafish NFE2 gene is adjacent to the HoxC cluster, similar to mapping studies in mouse and humans. As illustrated by the cloning of zebrafish NFE2, there is extensive conservation of the DNA-binding domain, whereas regions outside of these domains are less conserved. DNA-binding domains are important functional motifs, and recently these domains have also been shown to function as protein-protein interaction motifs. The lack of amino acid conservation in the putative activation domains of zebrafish and mammalian p45-NFE2 does not necessarily indicate lack of importance, and some structural characteristics may be conserved.

We find that p45-NFE2 expression is not detected in *cloche* mutant embryos. This is consistent with previous work showing that *cloche* is a gene that affects

COLOR

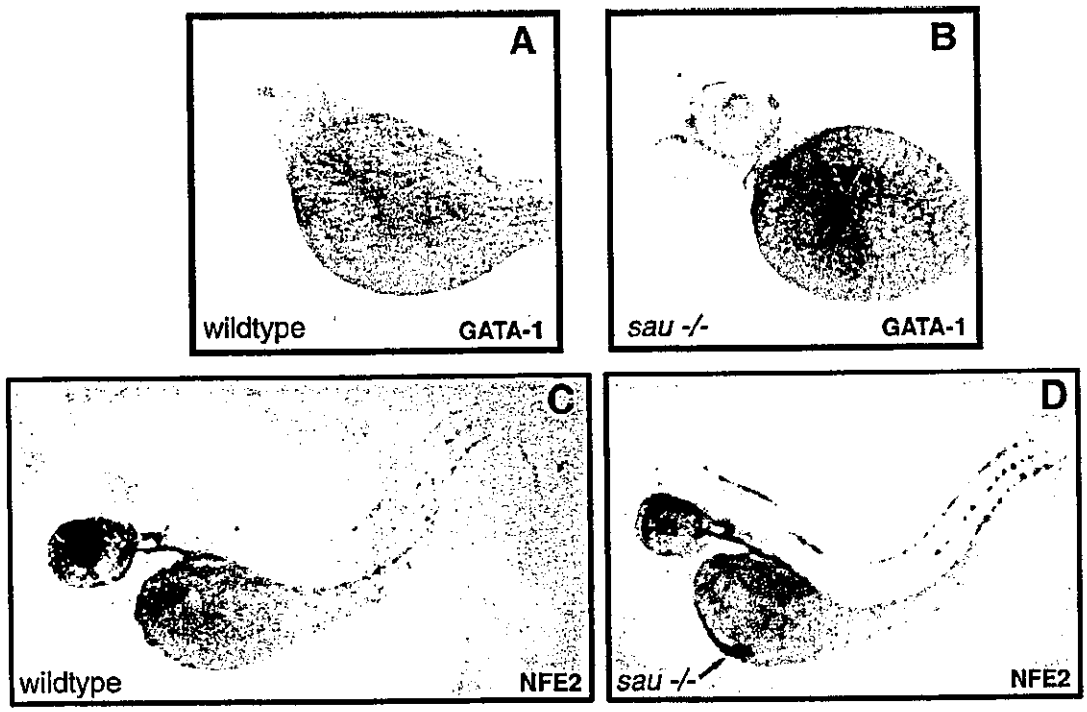

Fig. 5. In situ expression of erythroid markers in *sauternes* at 3 days postfertilization. Ventral view of GATA-1 expression in wild type (*A*) and *sauternes* (*B*). Lateral view of NFE2 expression in wild type (*C*) and *sauternes* (*D*).

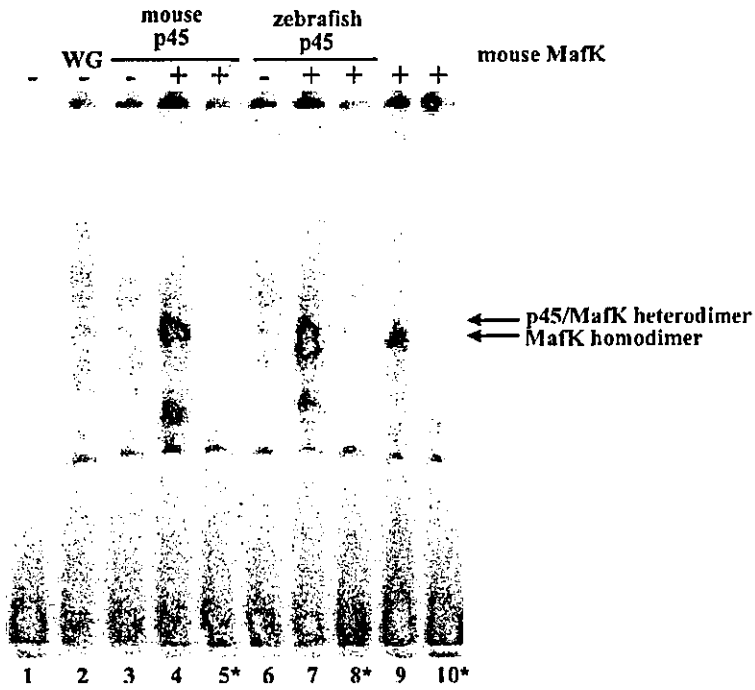

Fig. 6. Gel mobility shift analysis of zebrafish p45-NFE2 with mouse maf K. *Lanes 1–10*: labeled no. 25 DNA (250 pg) as a probe. **Lanes 5, 8, 10*: plus nonlabeled no. 25 DNA (100 ng) as a competitor. AQ: 15

hematopoietic stem cells, perhaps acting at the hemangioblast level. Other mutants could be studied for NFE2 expression, and it is likely some of the 26 complementation groups of zebrafish mutants will affect expression of this factor. In this regard, we analyzed the expression of NFE2 in *sauternes*, a mutant with heme deficiency (6). Our previous analyses of this mutant indicated that GATA-1 expression is abnormally maintained at a time when wild-type siblings show a downregulation. In this report, we found expression of NFE2 is also maintained in *sauternes* mutants. This suggests that heme deficiency leads to a defect in hematopoietic maturation and that this delays the normal downregulation of expression of the erythroid-specific transcription factors, NFE2 and GATA-1.

The isolation of zebrafish NFE2 demonstrates the conservation of the erythroid program among the vertebrates and supports an important role for this factor throughout evolution. The essential role of NFE2 may be in the generation of the thrombocyte lineage in the fish (19), which is functionally similar to the platelet lineage in mammalian biology. We have not yet evaluated the thrombocyte lineage in zebrafish for p45-NFE2 expression. p45-NFE2 may also have a role in erythroid development as evidenced by the murine knockout, although this role appears to be subtle (40). The conservation of the genomic location of NFE2 as adjacent to the Hox C cluster suggests that during the ancient tetraploidation of the vertebrate genome, the genes adjacent to the Hox clusters were maintained and utilized for distinct purposes (22). *nrf1* and *nfr2* are utilized for oxidative stress, whereas p45-NFE2 appears to be more relevant to hematopoietic differentiation. The zebrafish has a globin gene structure that includes α- and β-globins in the same locus (8). This structure is distinctly different from the mammalian globin loci. It is possible that p45-NFE2 could regulate globin gene expression, although locus control region elements have not been defined yet in the zebrafish system. Future work could assess the role of p45-NFE2 in hemoglobin switching in the zebrafish.

The zebrafish is an excellent forward genetic system for studying hematopoiesis. We have isolated factors by homology that are conserved throughout vertebrate evolution and are important in gene transcription. We have also defined the program by the study of 26 complementation groups of mutants that affect various differentiation processes (1, 36, 46). The availability of hematopoietic mutants allows for a defined characterization of the critical regulators of the blood program. Recent experiments using morpholinos, an antisense technology, offers an additional method for evaluating gene function (31). Characterization of zebrafish NFE2 using antisense or overexpression studies will provide a greater understanding of the function of this transcription factor during vertebrate hematopoiesis and should reinforce studies done in mammalian species. It will be interesting to evaluate the thrombocyte lineage with directed morpholinos to NFE2. As human diseases are mapped to genetic loci, the chromosomal synteny of the zebrafish should provide candidate genes for the study of human disease. For instance, the iron transporter, ferroportin-1, was isolated as a zebrafish mutant gene (27). Recently, mutations in the orthologous gene were detected in human patients with a rare form of hemochromatosis (29, 32). With the sequence of the zebrafish genome being done by the AQ: 11 AQ: 12

Sanger Center over the next 2 yr, additional information about the evolution of factors critical to hematopoiesis should be uncovered.

We thank Alan Davidson for reading this manuscript.

This work was supported by National Institutes of Health Grants R01-HL-48801-11, R01-DK-55381, and P50-DK-49216, as well as by Legal Sea Foods. L. I. Zon is an Investigator of the Howard Hughes Medical Institute.

AQ: 13

Editor S. L. Alper served as the review editor for this manuscript submitted by Editor L. I. Zon.

REFERENCES

1. **Amatruda J and Zon L.** Dissecting hematopoiesis and disease using the zebrafish. *Dev Biol* 216: 1–15, 1999.
2. **Andrews NC.** The NF-E2 transcription factor. *Int J Biochem Cell Biol* 30: 429–432, 1998.
3. **Andrews NC, Erdjument-Bromage H, Davidson MB, Tempst P, and Orkin SH.** Erythroid transcription factor NF-E2 is a haematopoietic-specific basic-leucine zipper protein. *Nature* 362: 722–728, 1993a.
4. **Andrews NC, Kotkow KJ, Ney PA, Erdjument-Bromage H, Tempst P, and Orkin SH.** The ubiquitous subunit of erythroid transcription factor NF-E2 is a small basic-leucine zipper protein related to the v-maf oncogene. *Proc Natl Acad Sci USA* 90: 11488–11492, 1993b.
5. **Andrews NC and Orkin SH.** Transcriptional control of erythropoiesis. *Curr Opin Hematol* 1: 119–124, 1994.
6. **Brownlie A, Donovan A, Pratt SJ, Paw BH, Oates AC, Brugnara C, Witkowska HE, Sassa S, and Zon LI.** Positional cloning of the zebrafish *sauternes* gene: a model for congenital sideroblastic anaemia. *Nat Genet* 20: 244–250, 1998.
7. **Caterina JJ, Donze D, Sun CW, Ciavatta DJ, and Townes TM.** Cloning and functional characterization of LCR-F1: a bZIP transcription factor that activates erythroid-specific, human globin gene expression. *Nucleic Acids Res* 22: 2383–2391, 1994.
8. **Chan FY, Robinson J, Brownlie A, Shivdasani RA, Donovan A, Brugnara C, Kim J, Lau BC, Witkowska HE, and Zon LI.** Characterization of adult α- and β-globin genes in the zebrafish. *Blood* 89: 688–700, 1997.
9. **Chan JY, Han XL, and Kan YW.** Cloning of Nrf1, an NF-E2-related transcription factor, by genetic selection in yeast. *Proc Natl Acad Sci USA* 90: 11371–11375, 1993.
10. **Chan JY, Kwong M, Lu R, Chang J, Wang B, Ten TSB, and Kan YW.** Targeted disruption of the ubiquitous CNC-bZIP transcription factor, Nrf-1, results in anemia and embryonic lethality in mice. *EMBO J* 17: 1779–1787, 1998.
11. **Chan K, Lu R, Chang JC, and Kan YW.** NRF2, a member of the NFE2 family of transcription factors, is not essential for murine erythropoiesis, growth, and development. *Proc Natl Acad Sci USA* 93: 13943–13948, 1996.
12. **Detrich HW, Kieran MW, Chan FY, Barone LM, Yee K, Rundstadler JA, Pratt S, Ransom D, and Zon LI.** Intraembryonic hematopoietic cell migration during vertebrate development. *Proc Natl Acad Sci USA* 92: 10713–10717, 1995.
13. **Donovan A, Brownlie A, Zhou Y, Shepard J, Pratt SJ, Moynihan J, Paw BH, Drejer A, Barut B, Zapata A, Law TC, Brugnara C, Lux SE, Pinkus GS, Pinkus JL, Kingsley PD, Palis J, Fleming MD, Andrews NC, and Zon LI.** Positional cloning of zebrafish ferroportin1 identifies a conserved vertebrate iron exporter. *Nature* 403: 776–781, 2000.
14. **Farmer SC, Sun CW, Winnier GE, Hogan BL, and Townes TM.** The bZIP transcription factor LCR-F1 is essential for mesoderm formation in mouse development. *Genes Dev* 11: 786–798, 1997.
15. **Goodfellow PN, Sefton L, and Farr CJ.** Genetic maps. *Philos Trans R Soc Lond B Biol Sci* 339: 139–146, 1993.
16. **Haffter P and Nusslein-Volhard C.** Large scale genetics in a small vertebrate, the zebrafish. *Int J Dev Biol* 40: 221–227, 1996.
17. **Igarashi K, Kataoka K, Itoh K, Hayashi N, Nishizawa M, and Yamamoto M.** Regulation of transcription by dimerization of erythroid factor NF-E2 p45 with small Maf proteins. *Nature* 367: 568–572, 1994.
18. **Jagadeeswaran P, Sheehan JP, Craig FE, and Troyer D.** Identification and characterization of zebrafish thrombocytes. *Br J Haematol* 107: 731–738, 1999.
19. **Johnson SL, Gates MA, Johnson M, Talbot WS, Horne S, Baik K, Rude S, Wong JR, and Postlethwait JH.** Centromere-linkage analysis and consolidation of the zebrafish genetic map. *Genetics* 142: 1277–1288, 1996.
20. **Kataoka K, Noda M, and Nishizawa M.** Maf nuclear oncoprotein recognizes sequences related to an AP-1 site and forms heterodimers with both Fos and Jun. *Mol Cell Biol* 14: 700–712, 1994.
21. **Kobayashi A, Ito E, Toki T, Kogame K, Takahashi S, Igarashi K, Hayashi N, and Yamamoto M.** Molecular cloning and functional characterization of a new cap'n'collar family transcription factor Nrf3. *J Biol Chem* 274: 6443–6452, 1999.
22. **Lecine P, Italiano, JE Jr, Kim SW, Villeval JL, and Shivdasani RA.** Hematopoietic-specific beta 1 tubulin participates in a pathway of platelet biogenesis dependent on the transcription factor NF-E2. *Blood* 96: 1366–1373, 2000.
23. **Levin J, Peng JP, Baker GR, Villeval JL, Lecine P, Burstein SA, and Shivdasani RA.** Pathophysiology of thrombocytopenia and anemia in mice lacking transcription factor NF-E2. *Blood* 94: 3037–3047, 1999.
24. **Li YJ, Higgins RR, Pak BJ, Shivdasani RA, Ney PA, Archer M, and Ben-David Y.** p45(NFE2) is a negative regulator of erythroid proliferation which contributes to the progression of friend virus-induced erythroleukemias. *Mol Cell Biol* 21: 73–80, 2001.
25. **Li YJ, Pak BJ, Higgins RR, Lu SJ, and Ben-David Y.** Contiguous arrangement of p45 NFE2, HnRNP A1, and HP1alpha on mouse chromosome 15 and human chromosome 12: evidence for suppression of these genes due to retroviral integration within the fli-2 locus. *Genes Chromosomes Cancer* 30: 91–95, 2001.
26. **Liao EC, Paw BH, Peters LL, Zapata A, Pratt SJ, Do CP, Lieschke G, and Zon LI.** Hereditary spherocytosis in zebrafish riesling illustrates evolution of erythroid β-spectrin structure, and function in red cell morphogenesis and membrane stability. *Development* 127: 5123–5132, 2000.
27. **Martin F, Deursen JMV, Shivdasani RA, Jackson CW, Troutman AG, and Ney PA.** Erythroid maturation and globin gene expression in mice with combined deficiency of NF-E2 and nrf-2. *Blood* 91: 3459–3466, 1998.
28. **Montosi G, Donovan A, Totaro A, Garuti C, Pignatti E, Cassanelli S, Trenor CC, Gasparini P, Andrews NC, and Pietrangelo A.** Autosomal-dominant hemochromatosis is associated with a mutation in the ferroportin (SLC11A3) gene. *J Clin Invest* 108: 619–623, 2001.
29. **Motohashi H, Katsuoka F, Shavit JA, Engel JD, and Yamamoto M.** Positive or negative MARE-dependent transcriptional regulation is determined by the abundance of small Maf proteins. *Cell* 103: 865–875, 2000.
30. **Nasevicius A and Ekker SC.** Effective targeted gene "knockdown" in zebrafish. *Nat Genet* 26: 216–220, 2000.
31. **Njajou OT, Vaessen N, Josse M, Berghuis B, van Dongen JW, Breuning MH, Snijders PJ, Rutten WP, Sandkuijl LA, Oostra BA, van Duijn CM, and Heutink P.** A mutation in SLC11A3 is associated with autosomal dominant hemochromatosis. *Nat Genet* 28: 213–214, 2001.
32. **Orkin SH and Zon LI.** Genetics of erythropoiesis: induced mutation in mice and zebrafish. *Annu Rev Genet* 31: 33–60, 1997.
33. **Oyake T, Itoh K, Motohashi H, Hayashi N, Hoshino H, Nishizawa M, Yamamoto M, and Igarashi K.** Bach proteins belong to a novel family of BTB-basic leucine zipper transcription factors that interact with MafK and regulate transcription through the NF-E2 site. *Mol Cell Biol* 16: 6083–6095, 1996.
34. **Postlethwait J, Yan Y, Gates M, Horne S, Amores A, Brownlie A, Donovan A, Egan E, Force A, Gong Z, Goutel C, Fritz A, Kelsh R, Knapik E, Liao E, Paw B, Ransom D, Singer A, Thomson M, Abduljabbar T, Yelick P, Beier D, Joly J, Larhammar D, Rosa F, Zon L, Johnson S, Westerfield M, and Talbot W.** Vertebrate genome evolution and the zebrafish gene map. *Nat Genet* 18: 345–349, 1998.

36. **Ransom DG, Haffter P, Odenthal J, Brownlie A, Vogelsang E, Kelsh RN, Brand M, van Eeden FJ, Furutani-Seiki M, Granato M, Hammerschmidt M, Heisenberg CP, Jiang YJ, Kane DA, Mullins MC, and Nusslein-Volhard C.** Characterization of zebrafish mutants with defects in embryonic hematopoiesis. *Development* 123: 311–319, 1996.
38. **Sayer MS, Tilbrook PA, Spadaccini A, Ingley E, Sarna MK, Williams JH, Andrews NC, and Klinken SP.** Ectopic expression of transcription factor NF-E2 alters the phenotype of erythroid and monoblastoid cells. *J Biol Chem* 275: 25292–25298, 2000.
39. **Shivdasani RA and Orkin SH.** Erythropoiesis and globin gene expression in mice lacking the transcription factor NF-E2. *Proc Natl Acad Sci USA* 92: 8690–8694, 1995.
40. **Shivdasani RA, Rosenblatt MF, Zucker-Franklin D, Jackson CW, Hunt P, Saris CJ, and Orkin SH.** Transcription factor NF-E2 is required for platelet formation independent of the actions of thrombopoietin/MGDF in megakaryocyte development. *Cell* 81: 695–704, 1995.
41. **Stainier DY, Weinstein BM, Detrich HW III, Zon LI, and Fishman MC.** Cloche, an early acting zebrafish gene, is required by both the endothelial and hematopoietic lineages. *Development* 121: 3141–3150, 1995.
43. **Talbot D and Grosveld F.** The 5'HS2 of the globin locus control region enhances transcription through the interaction of a multimeric complex binding at two functionally distinct NF-E2 binding sites. *EMBO J* 10: 1391–1398, 1991.
44. **Thompson MA, Ransom DG, Pratt SJ, MacLennan H, Kieran MW, Detrich, HW III, Vail B, Huber TL, Paw B, Brownlie AJ, Oates AC, Fritz A, Gates MA, Amores A, Bahary N, Talbot WS, Her H, Beier DR, Postlethwait JH, and Zon LI.** The cloche and spadetail genes differentially affect hematopoiesis and vasculogenesis. *Dev Biol* 197: 248–269, 1998.
45. **Tsang AP, Visvader JE, Turner CA, Fujiwara Y, Yu C, Weiss MJ, Crossley M, and Orkin SH.** FOG, a multitype zinc finger protein, acts as a cofactor for transcription factor GATA-1 in erythroid and megakaryocytic differentiation. *Cell* 90: 109–119, 1997.
46. **Weinstein BM, Schier AF, Abdelilah S, Malicki J, Solnica-Krezel L, Stemple DL, Stainier DY, Zwartkruis F, Driever W, and Fishman MC.** Hematopoietic mutations in the zebrafish. *Development* 123: 303–309, 1996.

Loss of the Nrf2 transcription factor causes a marked reduction in constitutive and inducible expression of the glutathione S-transferase *Gsta1*, *Gsta2*, *Gstm1*, *Gstm2*, *Gstm3* and *Gstm4* genes in the livers of male and female mice

Simon A. CHANAS*[1], Qing JIANG*[1], Michael McMAHON*, Gail K. McWALTER*, Lesley I. McLELLAN*, Clifford R. ELCOMBE*, Colin J. HENDERSON†, C. Roland WOLF†, Graeme J. MOFFAT‡, Ken ITOH§, Masayuki YAMAMOTO§ and John D. HAYES*[2]

*Biomedical Research Centre, Ninewells Hospital and Medical School, University of Dundee, Dundee DD1 9SY, Scotland, U.K., †Cancer Research UK, Molecular Pharmacology Unit, Ninewells Hospital, Dundee DD1 9SY, Scotland, U.K., ‡Syngenta Central Toxicology Laboratory, Alderley Park, Macclesfield, Cheshire SK10 4TJ, England, U.K., and §Centre for Tsukuba Advanced Research Alliance and Institute of Basic Medical Sciences, University of Tsukuba, Tsukuba 305-8577, Japan

Mice that lack the Nrf2 basic-region leucine-zipper transcription factor are more sensitive than wild-type (WT) animals to the cytotoxic and genotoxic effects of foreign chemicals and oxidants. To determine the basis for the decrease in tolerance of the *Nrf2* homozygous null mice to xenobiotics, enzyme assay, Western blotting and gene-specific real-time PCR (TaqMan®) have been used to examine the extent to which hepatic expression of GSH-dependent enzymes is influenced by the transcription factor. The amounts of protein and mRNA for class Alpha, Mu and Pi glutathione S-transferases were compared between WT and Nrf2 knockout (KO) mice of both sexes under both constitutive and inducible conditions. Among the class Alpha and class Mu transferases, constitutive expression of Gsta1, Gsta2, Gstm1, Gstm2, Gstm3, Gstm4 and Gstm6 subunits was reduced in the livers of *Nrf2* mutant mice to between 3% and 60% of that observed in WT mice. Induction of these subunits by butylated hydroxyanisole (BHA) was more marked in WT female mice than in WT male mice. TaqMan® analyses showed the increase in transferase mRNA caused by BHA was attenuated in $Nrf2^{-/-}$ mice, with the effect being most apparent in the case of Gsta1, Gstm1 and Gstm3. Amongst class Pi transferase subunits, the constitutive hepatic level of mRNA for Gstp1 and Gstp2 was not substantially affected in the KO mice, but their induction by BHA was dependent on Nrf2; this was more obvious in female mutant mice than in male mice. Nrf2 KO mice exhibited reduced constitutive expression of the glutamate cysteine ligase catalytic subunit, and, to a lesser extent, the expression of glutamate cysteine ligase modifier subunit. Little variation was observed in the levels of glutathione synthase in the different mouse lines. Thus the increased sensitivity of $Nrf2^{-/-}$ mice to xenobiotics can be partly attributed to a loss in constitutive expression of multiple GSH-dependent enzymes, which causes a reduction in intrinsic detoxification capacity in the KO animal. These data also indicate that attenuated induction of GSH-dependent enzymes in $Nrf2^{-/-}$ mice probably accounts for their failure to adapt to chronic exposure to chemical and oxidative stress.

Key words: antioxidant responsive element, cancer chemoprevention, carcinogenesis, detoxification, glutamate cysteine ligase (also called γ-glutamylcysteine synthetase).

INTRODUCTION

The ability to withstand toxic chemicals and oxidative stress is essential for the survival of all organisms. Various mechanisms have evolved to protect cells against foreign compounds and reactive oxygen species, including efflux pumps, antioxidant proteins and GSH, drug-metabolism, sequestration of toxins and DNA repair [1]. A number of genes encoding proteins involved in these processes can be induced by the compounds against which they provide protection, thereby enabling cells to survive exposure to harmful xenobiotics as well as oxidants [1,2].

One of the most versatile mechanisms of transcriptional adaptation to chemical stress involves the antioxidant-responsive element (ARE). This enhancer was first discovered because of its involvement in the inducible regulation of rat glutathione S-transferase class Alpha 2 (*GSTA2*) and rat NAD(P)H:quinone oxidoreductase 1 genes [3,4]. Deletion and mutation analyses of the promoter of rat *GSTA2* defined the ARE as 5′-(A/G)GTGACNNNGC-3′ [3]. This element responds to Michael reaction acceptors, hydroquinones, catechols, isothiocyanates, peroxides, trivalent arsenicals and heavy-metal salts [3,5,6]. The prototypic inducer of ARE-driven transcription is t-butylhydroquinone (t-BHQ), a major metabolite of the phenolic antioxidant butylated hydroxyanisole (BHA) [7].

The basic-region leucine-zipper (bZIP) factor Nuclear factor-erythroid 2 p45-related factor 2 (Nrf2), in combination with a small Maf protein, mediates transcriptional activation of genes via the ARE [8–11]. Evidence that Nrf2 confers protection against xenobiotics has been provided by studies of mice, or murine fibroblasts and macrophages, 'nulled' for this tran-

Abbreviations used: AGLN, α-angelicalactone; ARE, antioxidant-responsive element; BaP, benzo[a]pyrene; BHA, butylated hydroxyanisole; t-BHQ, t-butylhydroquinone; bZIP, basic-region leucine-zipper; CDNB, 1-chloro-2,4-dinitrobenzene; C+K, cafestol and kahweol palmitate; CMRN, coumarin; 3-OH CMRN, 3-hydroxy-CMRN; 7-OH CMRN, 7-hydroxy-CMRN; ECL, enhanced chemiluminescence; EQ, ethoxyquin; EST, expressed sequence tag; GCL(C), glutamate cysteine ligase (catalytic subunit); GCLM, GCL modifier subunit; GST, glutathione S-transferase; Gsta1/2, GST class Alpha 1/2; Gstm1/2/3/4/5/6, GST class Mu 1/2/3/4/5/6; Gstp1/2, Gst class Pi 1/2; I3C, indole-3-carbinol; KO, knockout; LMTN, limettin; Nrf2, Nuclear factor-erythroid 2 p45-related factor 2; OPZ, oltipraz; RACE, rapid amplification of cDNA ends; SUL, sulforaphane; WT, wild-type.

[1] These individuals contributed equally to this work, and should therefore be regarded as joint first authors.

[2] To whom correspondence and requests for reprints should be addressed (e-mail john.hayes@cancer.org.uk).

The nucleotide sequence data reported for mouse Gstm4 will appear in DDBJ, EMBL, GenBank® and GSDB Nucleotide Sequence Databases under the accession number AF501320.

scription factor. In mouse experimental models possessing disrupted *Nrf2*, increased sensitivity to 1-chloro-2,4-dinitrobenzene (CDNB) [12], acetaminophen [13,14], butylated hydroxytoluene [15], ethoxyquin (EQ) [16] and coumarin (CMRN) [16] has been observed. The $Nrf2^{-/-}$ mice are more susceptible to DNA adduct formation in target tissue when exposed to diesel-exhaust fumes [17], and during benzo[*a*]pyrene (BaP) carcinogenesis they develop more forestomach tumours than wild-type (WT) animals [18]. Loss of Nrf2 might also influence sensitivity to hyperoxic lung injury [19]. These phenotypic changes presumably occur either through altered expression of ARE-driven genes or failure to adapt to chemical/oxidative stress, or both.

In mice with targeted disruption of *Nrf2*, decreases have been reported in the constitutive and/or inducible expression of class Alpha, class Mu and class Pi glutathione S-transferases (GSTs), and the catalytic subunit of glutamate cysteine ligase (GCLC) [7,9,12–18,20]. These studies raise several important mechanistic questions. First, it is unclear precisely how Nrf2 exerts its pleiotropic effects *in vivo*, because among mouse genes encoding antioxidant and detoxication enzymes, only the promoter of *Gsta1* has been shown to contain a functional ARE; in *Gsta1*, a 41 bp DNA fragment that contains two tandemly arrayed 'core' ARE sequences has been referred to as an electrophile-responsive element [21]. It is therefore not known whether the effect of Nrf2 on other detoxication genes is direct, or whether it acts indirectly. It could, for example, induce other transcription factors. Secondly, within some of the superfamilies of drug-metabolizing enzymes the identities of genes regulated by Nrf2 is uncertain. Investigations into the phenotypic changes caused by disruption of *Nrf2* in the mouse have used Western blotting, Northern blotting and reverse-transcriptase PCR. These techniques cannot discriminate between gene products that share substantial sequence identity. In addition, these methods are at best only semi-quantitative. Thus it is not possible to determine whether the expression of Gsta1 or another class Alpha transferase (for example, Gsta2) is influenced by loss of Nrf2. Similar criticism can be levelled at data relating to class Mu GST and class Pi GST.

The lack of certainty about the identity of genes that are regulated by Nrf2 represents a major impediment to a rigorous understanding of why mice, or cell lines, nulled for the bZIP factor are sensitive to xenobiotics. Although, as described above, this problem is primarily due to the lack of specificity and accuracy in analytical techniques employed, problems with the nomenclature of class Mu GST genes causes a further layer of confusion. Specifically, in 1991, protein purification and amino acid sequencing revealed the presence in mouse hepatic cytosol of a BHA-inducible class Mu transferase subunit that was called Yb_5 [22]. This subunit was re-designated Gstm4* when the unified nomenclature devised for human GST was applied to the murine transferases [23], because it is distinct from the three class Mu transferases that had been described previously [24,25]. Thereafter, between 1995 and 1998 two further class Mu family members were identified in the mouse, both of which were called Gstm5 [26–28]. In the present study, we have used the term Gstm5 to describe the testis/brain-specific subunit reported by Fulcher et al. [26] and Rowe et al. [27], since this was the first of the two most recently characterized class Mu transferases to be cloned. We now refer to the remaining class Mu subunit that was reported by De Bruin et al. [28] as Gstm6.

The objective of the present study was to determine the role *in vivo* of Nrf2 in the expression of GST isoenzymes and the enzymes involved in GSH biosynthesis in livers of male and female mice. We first undertook cloning of the cDNA for Gstm4* to determine its entire primary structure, thereby allowing the nomenclature for the class Mu GST to be defined unambiguously. Subsequently, we developed gene-specific TaqMan® real-time PCR assays for all known murine mRNAs encoding class Alpha (Gsta1, Gsta2, Gsta3, Gsta4), class Mu (Gstm1, Gstm2, Gstm3, Gstm4, Gstm5, Gstm6) and class Pi (Gstp1, Gstp2) transferases. Similar assays were also established for GCLC and the glutamate cysteine ligase modifier subunit (GCLM; for a review of the function and regulation of GCL subunits, see [2]). Besides examining constitutive gene expression in $Nrf2^{-/-}$ and $Nrf2^{+/+}$ mice, induction by BHA has also been studied because, through metabolism to t-BHQ, it stimulates ARE-driven transcription [7].

MATERIALS AND METHODS

Chemicals

These were all of the highest purity that was commercially available, and the sources have been described in previous publications from our laboratories [16].

Animals

Throughout this study, mice were treated as recommended by regulations contained in the Animals and Scientific Procedure Act (1986) of the U.K. Generation of the $Nrf2^{-/-}$ mouse and genotyping of progeny has been described elsewhere [9,16].

Mice were housed at a temperature range of 19–23 °C under 12 h light/dark cycles. They were routinely fed *ad lib.* on RM1 laboratory animal feed (SDS Ltd, Witham, Essex, U.K.), and given free access to water. Mice of between 10 and 12 weeks of age were used for feeding experiments. These were each of 14 days' duration, and involved supplementing the RM1 diet as follows: BHA, 0.5 % (w/w) or 0.25 % (w/w); EQ, 0.25 % (w/w); oltipraz (OPZ), 0.075 % (w/w); indole-3-carbinol (I3C), 0.5 % (w/w); cafestol and kahweol palmitate (C+K), 0.025 % (w/w); sulforaphane (SUL), 3 μmol/g; coumarin (CMRN), 0.25 % (w/w); 3-hydroxy-CMRN (3-OH CMRN), 0.25 % (w/w); 7-hydroxy-CMRN (7-OH CMRN), 0.25 % (w/w); limettin (LMTN), 0.25 % (w/w); and α-angelicalactone (AGLN), 0.25 % (w/w).

Five separate feeding experiments were undertaken, each of 14 days' duration. In the first four experiments, male Nrf2 knockout (KO) and WT mice were fed the following diets: 1, control or BHA [at 0.5 % (w/w)]; 2, control, EQ, OPZ or I3C; 3, control, C+K or SUL; 4, control, CMRN, 3-OH CMRN, 7-OH CMRN, LMTN or AGLN. In experiment 5, both male and female Nrf2 KO and WT mice were fed either control or BHA [at 0.25 % (w/w)] diets.

Once the test-feeding period was complete, animals were killed by exposure to a rising concentration of CO_2, followed by cervical dislocation. Livers were removed and snap-frozen immediately in liquid N_2, before being stored at −70 °C.

Preparation of hepatic cytosol

Upon removal from the −70 °C freezer, portions (approx. 350 mg) of livers from each mouse were pulverized separately using a pestle and mortar under liquid N_2. The resulting finely ground material from each sample was resuspended in 4 ml of ice-cold 50 mM Hepes buffer, pH 7.5, containing 150 mM NaCl and 1 mM dithiothreitol. This buffer was fortified with Complete EDTA-free protease inhibitor at a dose of one tablet/50 ml buffer, as recommended by Roche Diagnostics Ltd (Lewes, East Sussex, U.K.). The pulverized hepatic material was placed on ice and homogenized mechanically by three separate 30 s pulses using an Omni homogenizer. The resulting extracts were subjected to two centrifugation steps at 4 °C (15000 *g* for 45 min,

Table 1 Oligonucleotide primers and probes for TaqMan® analyses

mRNA	Primers	Probe
Gsta1	forward: 5′-CCCCTTTCCCTCTGCTGAAG-3′ reverse: 5′-TGCAGCTTCACTGAATCTTGAAAG-3′	5′-TTCCTTGCTTCTTGAATTTGTTTTGCATCCAT-3′
Gsta2	forward: 5′-CCCCTTTCCCTCTGCTGAAG-3′ reverse: 5′-TGCAGCCACACTAAAACTTGAAAA-3′	5′-TTCCTTGCTTCTTCAATTTGTTTTGCATCCAA-3′
Gsta3	forward: 5′-TGGACAACTTCCCTCTCCTGAA-3′ reverse: 5′-AATCTTCTTTGCTGACTCAACACATT-3′	5′-TGAGAAGCAGAGTCAGCAACCTCCCCA-3′
Gsta4	forward: 5′-AACTTGTATGGGAAGGACCTGAA-3′ reverse: 5′-CCACGGCAATCATCATCATC-3′	5′-CCATCTGCATACATGTCAATCCTGACTCTCTC-3′
Gstm1	forward: 5′-CCTATGATACTGGGATACTGGAACG-3′ reverse: 5′-GGAGCGTCACCCATGGTG-3′	5′-CGCGGACTGACACACCCGATCC-3′
Gstm2	forward: 5′-CCTATGACACTAGGTTACTGGGACA-3′ reverse: 5′-CACTGGCTTCGGTCATAGTCA-3′	5′-CCGTGGGCTGGCTCACGCC-3′
Gstm3	forward: 5′-TATGACACTGGGCTATTGGAACAC-3′ reverse: 5′-GGGCATCCCCCATGACA-3′	5′-CGCGGACTGACTCACTCCATCCG-3′
Gstm4	forward: 5′-AGGCTATGGATGTCTCCAATCAG-3′ reverse: 5′-TCCAGGGAGCTGCTCCAA-3′	5′-CCACCTTCAGTTTCTCAAAGTCTGGGCTG-3′
Gstm5	forward: 5′-GCTGGACGTGAAATTCAAGCTA-3′ reverse: 5′-CGTTACTCTGGGTGATCTTGTTCTTC-3′	5′-CTGGACTTTCCTAACCTGCCCTACCTCATGG-3′
Gstm6	forward: 5′-CCTCCCAGATCAGCTGAAACTCTA-3′ reverse: 5′-TCAAGGACATCATAGACGAGGAAGT-3′	5′-TGCAAAGGTGATCTTGTCCCCTGCAA-3′
Gstp1	forward: 5′-GCAAATATGTCACCCTCATCTACACC-3′ reverse: 5′-GCAGGGTCTCAAAAGGCTTCA-3′	5′-AGGGCCTTCACGTAGTCATTCTTACCATTCTCATAGT-3′
Gstp2	forward: 5′-CAAATATGGCACCATGATCTACAGA-3′ reverse: 5′-GCAGGGTCTCAAAAGGCTTCA-3′	5′-AGGGCCTTCACGTAGTCATTCTTACCATTCTCATAGT-3′
GCLC	forward: 5′-GGCGATGTTCTTGAGACTCTGC-3′ reverse: 5′-TTCCTTCGATCATGTAACTCCCATA-3′	5′-AGGACAAACCCCAACCATCCGACC-3′
GCLM	forward: 5′-CACAGGTAAAACCCAATAGTAACCAAGT-3′ reverse: 5′-GTGAGTCAGTAGCTGTATGTCAAATTGTT-3′	5′-CTGGCCTCCTGCTGTGTGATGCC-3′

followed by 100000 *g* for 90 min). The final 100000 *g* supernatants (cytosols) were collected and retained for enzyme analyses.

Analytical biochemistry

Protein concentration was determined as described previously [16]. GST enzyme activity was estimated using CDNB as the substrate [16].

Western blotting

In all experiments, 4 μg of protein from different liver samples, along with a positive standard (usually 0.01 μg of immunogen) was subjected to SDS/PAGE in a Bio-Rad Mini-Protean II Cell apparatus (Bio-Rad Laboratories, Hemel Hempstead, Herts., U.K.). The electroblotting method used to transfer proteins from the SDS/PAGE-resolving gel to an Immobilon-P membrane, the blocking of free protein-binding sites on Immobilon-P and the various immunochemical reactions have been described elsewhere [16]. The final antibody complexes on Immobilon-P were visualized by enhanced chemiluminescence (ECL) and autoradiography.

To ensure that comparison between different liver samples was valid, SDS/PAGE was always performed in duplicate, with one of the gels being stained with Coomassie Blue to confirm equal loading. Following electroblotting, Immobilon-P membranes were routinely stained with Ponceau S to verify equal transfer of all samples.

Quantification of GST polypeptides

Levels of the various GST subunits in livers of *Nrf2*$^{-/-}$ and WT mice on control and BHA-containing diets were determined using a combination of affinity chromatography and reversed-phase HPLC. The class Alpha, Mu and Pi GSTs were isolated from hepatic cytosol (approx. 500 mg of protein) by chromatography on 1.6 cm × 8.0 cm columns of GSH–agarose that were equilibrated with 50 mM Tris/HCl, pH 7.5. After extensive washing of the affinity column to remove non-specifically bound protein, the GST isoenzymes were eluted isocratically in a single pool by elution of the affinity column with 20 mM GSH in 100 mM Tris/HCl, pH 9.0. Individual GST subunits were resolved by reversed-phase HPLC on a 0.46 cm × 25.0 cm Brownlee C_{18} reversed-phase column (7 μm particle size and 30 nm pore size), which was eluted in two stages with a 25–54 % gradient of acetonitrile in aq. 0.1 % (v/v) trifluoroacetic acid: from 0–5 min, the column was eluted with a linear gradient of 25–43 % acetonitrile, and the flow rate was increased from 0.1 ml/min to 1.0 ml/min; from 5–60 min, the column was eluted at 1.0 ml/min with a linear gradient of 43–54 % acetonitrile. The eluate from the HPLC column was monitored for absorbance at 214 nm, and the amount of each subunit was estimated from the peak area using molar absorption coefficients that have been calculated by Johnson et al. [29] for the rat transferases. Collation of results from various groups of workers [22,27,30,31] indicates the murine polypeptides are eluted from reversed-phase HPLC columns in the following order: Gstm3, Gstm1, Gstm2, Gsta3, Gstp1/2, Gstm5, Gsta1, Gsta2, Gstm4* (Yb_5) and Gsta4. Identification of these peaks is facilitated by the fact that the concentration of Gstp1 and Gstp2 in the livers of male mice greatly exceeds that found in livers of female mice [31,32].

Molecular cloning of Gstm4

Both bioinformatics and a nested PCR strategy were employed to clone Gstm4. Sense oligonucleotides specific for the 5′-untranslated region end of the cDNA (GM4F1, 5′-CCGGAG-

CCGGGGACTCA-3′; GM4F2, 5′-AGTCTCAGGCACCAG-CATC-3′) were designed following a personal communication from Dr William R. Pearson (University of Virginia, VA, U.S.A.), indicating that an IMAGE clone (GenBank® accession number AA538006) encodes part of Gstm4. Amplification of the cDNA was achieved using the sense oligonucleotides in two 3′ RACE (rapid amplification of cDNA ends) reactions. For this purpose, the oligo(dT) anchor primer was 5′-GACCACGCGTATCGA-TGTCGACTTTTTTTTTTTTTTTV-3′ (where V is A or G or C), and the anchor primer was 5′-GACCACGCGTATCGAT-GTCGAC-3′.

The cDNA for Gstm4 was amplified in two separate reactions. Total RNA from the liver of a male *Nrf2*$^{+/+}$ mouse on a control diet as template was isolated using an RNeasy kit (Qiagen Ltd., Crawley, West Sussex, U.K.). It was reverse-transcribed in the presence of oligo(dT)-anchor primer using SuperScript™ II (Gibco BRL, Life Technologies Ltd, Paisley, Scotland, U.K.) according to the supplier's instructions. The PCR was performed in 50 μl of reaction buffer containing approx. 100 ng of template DNA, 200 ng of each of the two oligonucleotides, 0.2 mM each of the four dNTPs and 1.25 units of *Pfu* Turbo® DNA polymerase (Stratagene, Amsterdam-Zuidoost, The Netherlands). In the first amplification reaction, the DNA template was subjected to an initial 94 °C denaturation step for 2 min. Thereafter, for the following 35 cycles, the DNA was denatured by heating at 94 °C for 45 s, the GM4F1 oligonucleotide and the oligo(dT)-anchor primer were allowed to anneal at 52 °C for 45 s, and elongation of the primers took place at 72 °C for 2 min. In the final cycle, the DNA was extended at 72 °C for 10 min to yield the first PCR products. An aliquot of this reaction mixture (1 μl) was diluted 1:10 before being subjected to a second nested PCR using GM4F2 and the same anchor primer oligonucleotides used in the first amplification reaction. The conditions employed for the second PCR were identical with those used for the first amplification, with the single exception that the primers were annealed at 55 °C in order to increase specificity.

Measurement of mRNA levels

This was performed using TaqMan® chemistry. The method first entailed cDNA synthesis from hepatic RNA, and this was followed by quantitative real-time PCR using the PerkinElmer/Applied Biosystems Prism Model 7700 Sequence Detector instrument.

Total RNA from livers of male and female *Nrf2*$^{-/-}$ and WT mice was prepared using RNeasy kits (Qiagen Ltd.). Contaminating genomic DNA was removed from 400 μg of RNA by on-column DNase digestion (Qiagen Ltd.). In each sample, single-stranded cDNA was synthesized using 100 units of Superscript II reverse transcriptase (Gibco BRL) and 0.15 μg of random hexamers (Promega UK, Chilworth, Southampton, U.K.) in a 20 μl solution of 50 mM Tris/HCl, pH 8.0, 75 mM KCl and 3 mM $MgCl_2$ containing 10 mM dithiothreitol and 1 mM dNTPs. The reaction mixture was left to equilibrate at 25 °C for 15 min before synthesis was allowed to proceed at 42 °C for 50 min. Finally, the reaction was terminated by incubation at 70 °C for 10 min, and the cDNA-containing reaction mixtures were diluted to 200 μl and stored at −20 °C until required.

Matching oligonucleotide primers and fluorescent probes used for real-time PCR were designed using the software Primer Express™ (PerkinElmer Applied Biosystems), and are listed in Table 1. The primers were synthesized by MWG-Biotech UK Ltd. (Milton Keynes, U.K.). The probes, which were labelled with a 5′ fluorescent reporter dye (6-carboxyfluorescein) and a 3′ quenching dye (6-carboxytetramethylrhodamine), were synthesized by Cruachem Ltd. (Glasgow, Scotland, U.K.). Each PCR mix (15 μl) contained between 10 and 15 ng of cDNA, 900 nM forward and reverse oligonucleotide primers and 200 nM probe in 1× (final concentration) TaqMan® Master Mix (PerkinElmer). Amplification of cDNA was performed over 41 cycles in the Prism Model 7700 Sequence Detector instrument. The first cycle was performed using 50 °C for 2 min, followed by 95 °C for 10 min. Cycles 2–41 were performed at 95 °C for 15 s, followed by 60 °C for 1 min. Reactions were monitored by measuring fluorescence at 518 nm with excitation at 494 nm. Each assay was performed in triplicate.

The specificity of PCR amplifications from the various sets of oligonucleotide primers was examined routinely by agarose-gel electrophoresis. In the case of highly similar GST mRNAs, the specificity of the TaqMan® reactions was checked by using serial dilutions of several different authentic cDNAs as template.

The TaqMan® software was used to calculate a C_t value for each reaction; this value represents the extension phase of PCR, where the fluorescence signal produced by the amplified product can be distinguished from background. The level of 18 S ribosomal RNA was used as an internal standard (using a kit from PerkinElmer).

RESULTS

Identification of the cDNA for Gstm4* and definition of nomenclature for murine class Mu GST

The class Mu Gstm4* subunit, originally called Yb_5, was first purified as a heterodimer with Gstm1 from the livers of mice fed on a BHA-containing diet, and its C-terminal 198–218 residues

A

	Reference	Primary structure	Identity (%)
Yb_5	22	MKTSRFLRTPLYTKVATWGNK	
Gstm1	24,25	MKSSRYIATPIFSKMAHWSNK	52
Gstm2	25	MKSSRFLSKPIFAKMAFWNPK	52
Gstm3	24	MKSSRFLPRPVFTKIAQWGTD	57
Gstm4	AK003418	MKTSRFLRTPLYTKVATWGNK	100
Gstm5	26	LQSDRFFKMPINNKMAKWGNK	43
Gstm6	28	MKTSRFLPSPVYLKQATWGNE	71

B

	Reference	Primary structure	Identity (%)
Yb_5	22	MDDSNQLARVXYSPDFEKLKVEYLEQ	
Gstm1	24,25	MDTRMQLIMLCYNPDFEKQKPEFLKT	52
Gstm2	25	MDTRIQLAMVCYSPDFEKKKPEYLEG	72
Gstm3	24	MDTRIQLMIVCCSPDFEKQKPEFLKA	56
Gstm4	AK003418	MDVSNQLARVCYSPDFEKLKVEYLEQ	96
Gstm5	26	MDFRMQLVRLCYNSNHENLKPQYLEQ	52
Gstm6	28	MDTRIQMGMLCYSADFEKRKPEFLKG	48

Figure 1 Comparison between sequences of CNBr peptides generated from Yb_5 and equivalent regions of other class Mu GST

(**A**) The sequence of the Yb_5 CNBr-a peptide described by Hayes et al. [22], is shown aligned with residues 198–218 of class Mu transferases; the numbering of the residues includes the initiator methionine, but not the four-amino-acid N-terminal extension that is unique to mouse Gstm5. The reference provided against the murine class Mu transferases represents the first description of the cDNA clone for individual subunits. The entry against Gstm4 represents the RIKEN cDNA 1110004G14 (accession number AK003418). (**B**) The sequence of the Yb_5 CNBr-d peptide [22] is shown aligned with residues 105–130 of class Mu GST.

```
 M  P  M  T  L  G  Y  W  D  I  R  G  L  A  H  A  I  R  L  L     20
atgcctatgacactgggttactgggacatccgtgggctagctcacgctattcggctgctc     60

 L  E  Y  T  G  S  S  Y  E  E  K  R  Y  T  M  G  D  A  P  D     40
ctagaatacacaggctcaagctatgaagagaagagatacaccatgggagacgctcctgac    120

 Y  D  R  S  Q  W  L  S  E  K  F  K  L  G  L  D  F  P  N  L     60
tatgaccgaagccagtggctgagtgagaagttcaaattgggcctggactttcccaatttg    180

 P  Y  L  I  D  G  S  H  K  I  T  Q  S  N  A  I  L  R  Y  I     80
ccttacttgattgatgggtcacacaagatcacgcagagcaatgccatcctgcgctacatt    240

 A  R  K  H  N  L  C  G  E  T  E  E  E  K  I  R  V  D  I  L    100
gcccgcaagcacaacctgtgtggggagacagaggaagagaagattcgcgtggacattttg    300

 E  N  Q  A  M  D  V  S  N  Q  L  A  R  V  C  Y  S  P  D  F    120
gagaaccaggctatggatgtctccaatcagctggctcgagtctgttacagcccagacttt    360

 E  K  L  K  V  E  Y  L  E  Q  L  P  G  M  V  K  L  F  S  Q    140
gagaaactgaaggtggaatacttggagcagctccctggaatggtgaagctcttctcacag    420

 F  L  G  Q  R  T  W  F  V  G  E  K  I  T  F  V  D  F  L  A    160
ttcctgggccagcggacatggtttgttggtgaaaagattacttttgtagatttcctggct    480

 Y  D  I  L  D  L  H  L  I  F  E  P  T  C  L  D  A  F  P  N    180
tacgatatcctggacctgcaccttatattcgaacccacgtgcctggacgccttcccaaac    540

 L  K  D  F  V  A  R  F  E  V  L  K  R  I  S  A  Y  M  K  T    200
ctgaaggactttgtggcccgctttgaggtactgaagaggatctctgcttacatgaagacc    600

 S  R  F  L  R  T  P  L  Y  T  K  V  A  T  W  G  N  K  -       218
agccgcttcctccgaacacccctatatacaaaggtggccacttggggcaataagtagagc    660

cttgactgggcaggaagtgggaaccgggggttctgggaacagttgaacttcctgtagccc    720
tagtgctgctttctgtccatcccctttcctgaccccagagtgtcaaaggtcctcttttctt    780
tcatccagtccctgccctttcaaaccctctaaagcctaggctcctagttttcctttagca    840
aaatgcccttctagcatgactgtgtcccgcgcccacttgatggtcttgcctgccagcagc    900
tgtgctgttgtgaagagttgggactctccatcagcactcagcctggggctccccatgctt    960
gtctggagaccagagacggctggtgtgtgaatttggtctctgcacagctcttttgggtcc   1020
ctcctgtaaagcctgaaccacactggctctggctgccgcactaccagcttttactactat   1080
ctccagtggctgcctagtgacccgggcagaggctgagttcacagggattttagttggata   1140
ggcaggggtttggcccttcctagccccacctgtttgtttctcaggaggcagctgcagaag   1200
gctctgtggagctcaaagggagcttagatctcctttatgctagcagcactgagatttgtc   1260
atgcaggtctcagtggtgaggatccaggctgataggagtccccagcagaaagccaggatc   1320
ctctctgcccactgtgctatggctgccttatatctatatgtctccaggatcctgtctctg   1380
atgtcttcagagtatcccgtcttggtcaccagggatgggggccatcttggttaatccctc   1440
ctctttgtgagcccccgtgaataaaatttcttcatgctttcggaaaaaaaa            1491
```

Figure 2 Nucleotide and deduced primary protein structure of murine Gstm4

Table 2 GST activities in the cytosolic fraction of mouse liver

GST activity is expressed as μmol/min per mg of GST with CDNB as substrate. The values presented represent mean catalytic activities ($\pm$S.E.M.) from triplicate measurements of pooled hepatic cytosol from three separate animals. The numbers in parentheses represent the mean activity value as a percentage of the value obtained with *Nrf2*$^{+/+}$ on a control diet within the same experimental group.

	GST activity	
Genotype ...	*Nrf2*$^{+/+}$	*Nrf2*$^{-/-}$
Diet		
Control 1	6.7 $\pm$ 0.1 (100)	4.4 $\pm$ 0.1 (66)
BHA*	23.9 $\pm$ 0.2 (357)	4.2 $\pm$ 0.2 (63)
Control 2	5.8 $\pm$ 0.4 (100)	2.8 $\pm$ 0.1 (48)
EQ	21.1 $\pm$ 0.1 (364)	4.8 $\pm$ 0.2 (83)
OPZ	16.1 $\pm$ 0.5 (278)	2.7 $\pm$ 0.1 (47)
I3C	9.9 $\pm$ 0.1 (171)	3.9 $\pm$ 0.1 (67)
Control 3	6.9 $\pm$ 0.1 (100)	3.4 $\pm$ 0.1 (49)
SUL	5.6 $\pm$ 0.1 (81)	2.9 $\pm$ 0.1 (42)
K + C	6.4 $\pm$ 0.1 (93)	3.1 $\pm$ 0.1 (45)
Control 4	5.9 $\pm$ 0.1 (100)	3.3 $\pm$ 0.1 (56)
CMRN	11.1 $\pm$ 0.1 (188)	3.3 $\pm$ 0.1 (56)
3-OH CMRN	5.0 $\pm$ 0.1 (85)	3.1 $\pm$ 0.1 (53)
7-OH CMRN	4.9 $\pm$ 0.1 (83)	3.3 $\pm$ 0.1 (56)
LMTN	12.2 $\pm$ 0.5 (207)	4.4 $\pm$ 0.1 (75)
AGLN	8.7 $\pm$ 0.1 (147)	3.4 $\pm$ 0.1 (58)

* In this experiment, BHA was administered at 0.5% (w/w) in the RM1 animal feed.

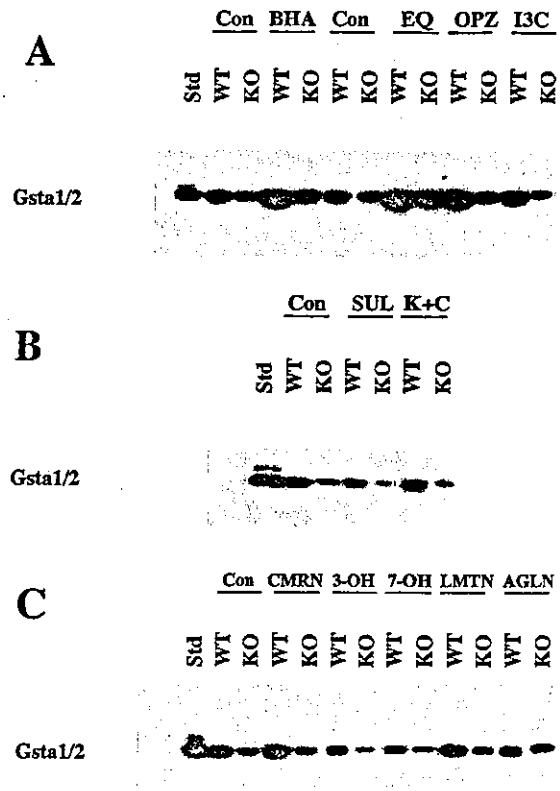

Figure 3 Constitutive and inducible Gsta1/2 protein levels in the liver of WT and *Nrf2* mutant mice fed on diets containing different xenobiotics

Both *Nrf2*$^{+/+}$ and *Nrf2*$^{-/-}$ mice were fed on diets supplemented with synthetic chemopreventive agents or phytochemicals, as described in the Materials and methods section. Portions (4 μg of protein) of cytosol from liver of WT and KO mice were subjected to Western blotting. Equality in the loading of protein from different samples was verified after electrophoresis by inspecting the intensity of Coomassie Blue staining of polyacrylamide gels, and of Ponceau S staining of Immobilon-P membranes. ECL located immunochemically cross-reacting polypeptides, and the results were visualized by autoradiography. Results from experiments 1 and 2 are shown in (**A**), whereas results from experiments 3 and 4 are shown in (**B**) and (**C**) respectively. The dietary supplements are indicated at the top of each panel. Affinity-purified rat liver GST was included as a standard (Std) in lane 1 of the gel. The genotype of each group of mice, WT and homozygous *Nrf2* mutant (KO) mice, is shown above the appropriate lane. The results presented are typical of those obtained; they were repeated on at least three separate occasions. Closely similar patterns of cross-reacting proteins were produced when the blots were repeated. Con, control.

were sequenced following cleavage with CNBr [22]. The C-terminal CNBr peptide from Gstm4* was used for a BLAST search of cDNA databases, because this region of class Mu GST polypeptides is divergent [27]. The CNBr peptide gave a 100% match with a hypothetical mouse protein encoded by a RIKEN cDNA (1110004G14; accession number AK003418) cloned from the mRNA of an 18-day-old C57BL/6J mouse embryo (Figure 1A). By contrast, the CNBr peptide was found to share between 43% and 72% identity with the equivalent C-terminal regions of murine Gstm1, Gstm2, Gstm3, Gstm5 and Gstm6. An additional CNBr peptide representing residues 105–130 of Gstm4* was also aligned with the protein encoded by the RIKEN cDNA clone. Although this contained one mismatch with the predicted amino acid sequence of the equivalent peptide in Gstm4, at least seven differences were observed when the CNBr peptide was compared with the amino acid sequence of the equivalent region in other mouse class Mu GSTs (Figure 1B).

The published RIKEN expressed sequence tag (EST) sequence for the putative Gstm4* (AK003418) appeared to lack nucleotides encoding the N-terminus of the protein. According to information provided by Dr William R. Pearson, the N-terminal region of Gstm4 was considered to be likely to be encoded by IMAGE clone 930982 (AA538006). A 3′-RACE approach was therefore adopted to isolate a cDNA containing the entire coding region of Gstm4*. This was achieved using RNA isolated from male *Nrf2*$^{+/+}$ mice fed on a control diet using an oligo(dT)-anchor primer targeted to the polyadenylated [poly(A)$^+$] tail of the message, and sense oligonucleotides found in the partial-length IMAGE clone aa538006, as described above. Figure 2 shows the cDNA sequence of Gstm4 and the predicted translated product. The determination of the full coding sequence for Gstm4 obviates the need for the asterisk in the subunit designation, and it is omitted hereafter.

It was noted originally that Gstm4 cross-reacted with antibodies raised against the rat GSTM5 subunit [22]. Therefore positive immunoblots of mouse tissues that have been generated by probing with anti-rGSTM5 (see [7] and [16]) could be due to cross-reactivity with either murine Gstm4 or Gstm5. Thus, in the blots presented below, cross-reactivity with anti-rat GSTM5 is labelled Gstm4/5.

BHA represents a potent inducer of class Alpha GST subunits in mouse liver

Before examining the regulation of hepatic detoxification and antioxidant genes in WT and Nrf2 KO mice of both sexes, an initial investigation was undertaken to identify which chemopreventive agent might serve as the best model inducer of these genes in the liver. For this purpose, the series of livers that was generated during the study of McMahon et al. [16] into induction of detoxication proteins in the small intestine of WT and Nrf2 KO mice was examined. It should be noted that this series comprised only livers from male mice.

Table 2 shows that increases in GST activity of between 1.7-fold and 3.6-fold were observed in the livers of WT mice fed on diets containing BHA, EQ, OPZ, I3C, CMRN, LMTN or

Table 3 GST activity in male and female mouse hepatic cytosol

GST activity is expressed as μmol/min per mg of protein for GST. The values presented represent mean catalytic activities ($\pm$S.E.M.) from triplicate measurements of pooled hepatic cytosol from three separate animals. The numbers in parentheses represent the mean activity value as a percentage of the value obtained with *Nrf2*$^{+/+}$ on a control diet within the same experimental group.

		GST activity	
Sex/diet	Genotype ...	*Nrf2*$^{+/+}$	*Nrf2*$^{-/-}$
Male/control 5		3.4 $\pm$ 0.1 (100)	1.2 $\pm$ 0.1 (35)
Male/BHA*		7.0 $\pm$ 1.1 (206)	1.1 $\pm$ 0.2 (32)
Female/control 5		1.5 $\pm$ 0.1 (100)	0.7 $\pm$ 0.01 (46)
Female/BHA*		9.6 $\pm$ 0.5 (640)	1.1 $\pm$ 0.1 (73)

* In this experiment, BHA was included at 0.25% (w/w) in the diet.

AGLN. In Nrf2-nulled mice, inclusion of the xenobiotics in the diet had essentially no effect on hepatic transferase activity.

Immunoblotting of hepatic cytosols from male WT mice revealed that feeding these animals on diets containing BHA, EQ, OPZ, CMRN, LMTN or AGLN resulted in substantial increases in Gsta1/2 subunits (Figure 3). By comparison, Western blotting with antibodies raised against mouse Gstm1-1, rat GSTM5-5 and mouse Gstp1-2 showed a less obvious increase in the transferase subunits in livers of male mice fed on diets containing the various xenobiotics (results not shown).

Dependence on Nrf2 for constitutive and inducible hepatic GST activities is apparent in both sexes

Having demonstrated that BHA is one of the more potent inducing agents among those readily commercially available, it was decided to examine induction by this antioxidant in both male and female mouse liver. The decision to study induction in male and female mice was taken because the expression of Pi class GST is sexually dimorphic in mouse liver [31,32], and induction of the transferases can vary in male and female mice [33]. The possibility that the hepatic levels of detoxication and antioxidant proteins are dependent on Nrf2 in a sex-specific fashion was therefore considered.

GST activity was lower in the livers from female WT mice fed on a control diet than in male mice supplied with the same food (Table 3). This sex difference in constitutive hepatic GST activity was still apparent in the KO animals, but in both females and males on a control diet the CDNB–GSH-conjugating activity in the liver was diminished. Transferase activity in the livers of female WT mice treated with BHA was increased to a greater extent than in males. However, only a modest induction of GST activity by BHA was observed in the livers of female Nrf2 KO mice.

Sex-specific effects of BHA on GST proteins in livers from *Nrf2*$^{+/+}$ and *Nrf2*$^{-/-}$ mice

Constitutive amounts of the class Alpha Gsta1/2 subunits were similar in livers from male and female WT mice. The livers of male *Nrf2*$^{-/-}$ mice, but not female *Nrf2*$^{-/-}$ mice, showed a modest reduction in the constitutive levels of Gsta1/2. In agreement with previous work, these subunits were found to be induced in the livers of WT mice placed on a BHA-containing diet. A comparison between the hepatic levels of Gsta1/2 in male and female *Nrf2*$^{-/-}$ mice fed on a control diet with genetically similar mice fed on a BHA-containing diet suggests that these

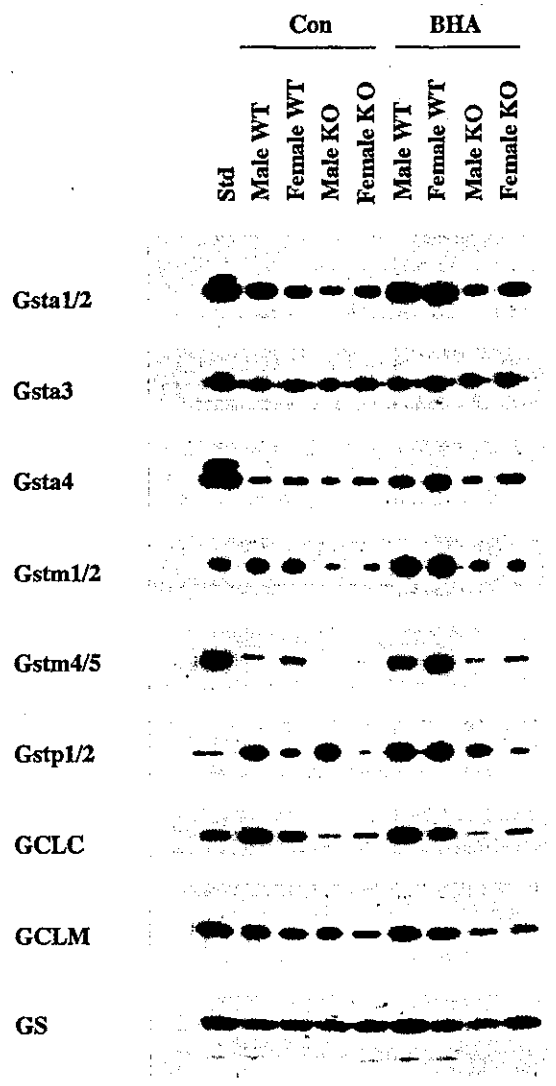

Figure 4 Nrf2 influences the constitutive and inducible expression of detoxication and antioxidant proteins in the livers of both male and female mice

Male and female Nrf2 WT and male and female Nrf2 KO mice were fed on either the RM1 control diet or RM1 diet containing 0.25% (w/w) BHA for 14 days. Hepatic extracts were prepared and portions (4 μg of protein) were examined by Western blotting, as described above. Protein loading was checked as described in the legend to Figure 3. The dietary treatments are shown at the top of the Figure. All gels were loaded in a similar fashion, and the identity of the samples applied to each lane is indicated above the autoradiogram for Gsta1/2. The identity of the murine proteins that are known to cross-react with the antiserum used to probe each blot is indicated in the left-hand margin. In lane 1 of each blot, a positive standard (Std) was included. For class Alpha transferases and Gstm1/2, affinity-purified rat liver GST was used as a standard; for Gstm4/5, affinity-purified mouse testis transferases were used as standard; for Gstp1/2, affinity-purified rat lung GST was used as standard. For GCL, rat kidney cytosol was used as the standard. For GS, recombinant protein served as standard.

class Alpha subunits are modestly inducible in the KO animals of both sexes (Figure 4).

Western blotting revealed little difference in the hepatic level of Gsta3 in male and female WT mice placed on either control or BHA diets. In livers of male *Nrf2*$^{-/-}$ mice fed on a control diet, there was evidence that Gsta3 was expressed in lower amounts than in WT control livers. The Gsta4 subunit was found consistently to be present in slightly higher amounts in livers of

Table 4 Quantification of GST subunits in mouse liver by HPLC

The transferases that were purified from mouse liver by affinity chromatography on columns of GSH–agarose were subjected to reversed-phase HPLC on a Brownlee C_{18} column, and quantified as described in the Materials and methods section. The BHA was supplied at 0.25% (w/w) in the RM1 laboratory animal feed. nd, not determined (insufficient material).

		Level of glutathione *S*-transferase subunits (mg/g cytosolic protein)*						
Sex and genotype	Diet	Gsta1/2†	Gsta3	Gsta4	Gstm1	Gstm2	Gstm4	Gstp1/2‡
Male, $Nrf2^{+/+}$	Control	n.d.	10.7	0.50	8.10	0.13	0.14	16.5
Male, $Nrf2^{-/-}$	Control	n.d.	2.8§	0.09§	0.83§	0.05	n.d.	17.5
Male, $Nrf2^{+/+}$	BHA	0.40	11.9§	0.62§	40.7§	4.40§	0.62§	31.7§
Male, $Nrf2^{-/-}$	BHA	n.d.	5.2§	0.17§	1.98§	0.10	n.d.	14.5
Female, $Nrf2^{+/+}$	Control	n.d.	11.7	0.54	10.6	0.44	n.d.	3.8
Female, $Nrf2^{-/-}$	Control	n.d.	7.7‖	0.27‖	1.19‖	0.09	n.d.	1.7‖
Female, $Nrf2^{+/+}$	BHA	1.12	11.1	0.84	70.0‖	11.40	0.95	15.3‖
Female, $Nrf2^{-/-}$	BHA	n.d.	8.2	0.45	2.44‖	0.36	0.07	3.1

* The mean value from three separate HPLC analyses of affinity-purified GST obtained from three different livers. The statistical significance of the data was determined using ANOVA followed by the Newman–Keuls test.

† The Gsta1 and Gsta2 subunits from mouse liver exhibit poor affinity for the GSH–agarose chromatography matix [34], and therefore the Gsta1/2 subunit levels in the Table are underestimates.

‡ The Gstp1 and Gstp2 subunits cannot be resolved by reversed-phase HPLC. Thus the data in this Table relating to these subunits are combined.

§ Comparison with male WT control gives a P value of < 0.001 by Newman–Keuls test.

‖ Comparison with female WT control gives a P value of < 0.001 by Newman–Keuls test.

female WT mice that those of male WT mice, and again the constitutive level of Gsta4 was found to be lower in the KO mice.

Mu class Gstm1/2 subunit(s) did not demonstrate sex-specific differences in mouse liver, although both the constitutive and inducible levels of Gstm1/2 were dependent on Nrf2 (Figure 4). The Gstm4/5 polypeptide(s) were expressed at higher levels in livers from female WT and female Nrf2 KO mice than in livers from genetically equivalent male animals. In WT mice of both sexes, Gstm4/5 was found to be inducible by BHA, with higher levels of the protein in livers of female animals still being apparent.

Under normal dietary conditions the Gstp1/2 subunit(s) was present at substantially lower amounts in livers from female WT mice than in livers from male mice. In $Nrf2^{-/-}$ mice fed on a control diet, the sex-specific expression of Pi class GST was still obvious. Indeed, constitutive hepatic expression of Gstp1/2 appeared to be diminished in mutant female mice, but not in male mice. Figure 4 shows that, in livers of female WT mice, the relative increase in Gstp1/2 affected by BHA treatment is much greater than is the case in livers from male mice. The increase in protein is sufficient to largely obscure the sexual dimorphism in this GST class. Treatment of $Nrf2^{-/-}$ mice with BHA did not cause a large induction of Pi class GST. Thus livers from female mutant mice fed BHA contained significantly lower levels of Gstp1/2 protein than did livers from male mice.

Effects of Nrf2 on GSH-biosynthetic proteins in mouse liver

Antibodies against enzymes involved in GSH biosynthesis were used to probe liver samples from female and male mice. As has been noted before in the mouse small intestine [16], significant inter-individual variation in the level of GCLC (previously called GCS_h) was also observed in the murine hepatic samples. Livers from female and male mice did not contain major differences in their levels of GCLC. BHA did not induce this subunit significantly in mouse liver. However, the constitutive level of GCLC in livers from both female and male mice was dependent on Nrf2 (Figure 4). The GCLM subunit did not show evidence of sexual dimorphism in mouse liver, nor was it found to be inducible by BHA. Constitutive expression of GCLM was modestly reduced in the Nrf2 KO mice (Figure 4). Neither sex nor Nrf2 or inducing agent influenced the expression of glutathione synthetase in mouse liver.

Regulation of GST subunits by Nrf2 in mouse liver from both sexes

Affinity chromatography and HPLC were employed to quantify individual transferase subunits in mouse liver. On the basis of protein recovery from GSH–agarose, it was calculated that, in male WT mice fed on a control diet, the GST pool represented 3.6% of the total hepatic cytosolic protein. In female mice fed on a control diet, the GST pool represented 2.7% of the hepatic cytosolic protein. These data are similar to previous calculations of the hepatic GST content in DBA/2, C3H/He and C57BL6 mice [32]. Reversed-phase HPLC resolved seven GST-containing peaks from the pools of affinity-purified hepatic transferases. These were identified by their order of elution as Gstm1, Gstm2, Gsta3, Gstp1/2, Gsta1/2, Gstm4 and Gsta4. In addition, the Gstm3 subunit was eluted at 14 min as a minor (< 0.5% of affinity-purified GST pool) incompletely resolved peak, immediately in front of Gstm1, and it was not quantified. Two other equally minor peaks that are thought to represent Gstm5 and Gstm6 were also observed, but were not quantified: Gstm5 eluted at 39 min between Gstp1/2 and Gsta1/2; Gstm6 eluted at 17 min immediately after Gstm2.

The Gsta1 and Gsta2 homodimers from mouse liver cytosol fail to bind GSH–agarose [34], and, although Table 4 shows the subunits are induced by BHA, the values presented are underestimates, since the majority of these subunits will not have been present in the GST pool analysed by HPLC. A modest reduction in the level of Gsta3 was observed in the livers of male $Nrf2^{-/-}$ mice when compared with male $Nrf2^{+/+}$ mice. Similar differences in hepatic Gsta3 were also apparent when female KO mice were compared with female WT mice, but the influence of Nrf2 on constitutive expression of the transferase is less obvious than in the male.

Major differences were found in the amount of hepatic Gstm1 in WT and KO mice of either sex. The level of Gstm1 in livers of $Nrf2^{-/-}$ mice fed on a control diet was only 10% of that in WT mice (Table 4). Furthermore, whereas BHA increased the levels of Gstm1 approx. 6-fold in male and female WT mice, the

Table 5 Quantification of hepatic mRNA for GST and GCL in WT and *Nrf2*$^{-/-}$ mice fed on either a control diet or one containing BHA

In each experimental group, total RNA from the livers of three different mice was combined and mRNA was quantified by TaqMan® using 18 S RNA as an internal standard. Each assay was performed in triplicate on at least two separate occasions. The values presented represent means ± S.E.M. mRNA levels, and are expressed as a ratio of the amount measured in the liver of *Nrf2*$^{+/+}$ mice of the same sex that were fed on a control diet. Comparison between the sexes revealed that the level of mRNA for Gsta1, Gstm4, Gstm6, Gstp1 and Gstp2 was 3.4-, 2.6-, 4.2-, 5.4- and 4.3-fold higher respectively in the livers of male WT mice fed on a control diet than in the livers of female WT mice. The control diet was RM1 animal feed, and BHA was provided in the RM1 diet at a dose of 0.25% by weight.

		Levels of mRNA encoding ...						
Sex and genotype	Diet	Gsta1	Gsta2	Gsta3	Gsta4	Gstm1	Gstm2	Gstm3
Male, Nrf2$^{+/+}$	Control	1.00 ± 0.09	1.00 ± 0.10	1.00 ± 0.11	1.00 ± 0.23	1.00 ± 0.12	1.00 ± 0.10	1.00 ± 0.13
Male, Nrf2$^{-/-}$	Control	0.03 ± 0.01	0.06 ± 0.01	0.32 ± 0.04	0.42 ± 0.08	0.12 ± 0.02	0.35 ± 0.04	0.11 ± 0.01
Male, Nrf2$^{+/+}$	BHA	15.65 ± 3.00	4.67 ± 0.13	0.95 ± 0.07	1.62 ± 0.12	3.57 ± 0.21	2.76 ± 0.14	12.38 ± 1.30
Male, Nrf2$^{-/-}$	BHA	0.73 ± 0.07	1.97 ± 0.13	1.29 ± 0.15	1.69 ± 0.18	0.63 ± 0.08	2.88 ± 0.27	2.26 ± 0.26
Female, Nrf2$^{+/+}$	Control	1.00 ± 0.21	1.00 ± 0.40	1.00 ± 0.24	1.00 ± 0.16	1.00 ± 0.12	1.00 ± 0.14	1.00 ± 0.12
Female, Nrf2$^{-/-}$	Control	0.13 ± 0.04	0.16 ± 0.02	0.78 ± 0.10	0.72 ± 0.08	0.17 ± 0.01	0.45 ± 0.05	0.10 ± 0.01
Female, Nrf2$^{+/+}$	BHA	124.5 ± 9.0	4.29 ± 0.06	2.24 ± 0.17	1.79 ± 0.31	7.28 ± 0.43	7.19 ± 0.19	61.18 ± 3.45
Female, Nrf2$^{-/-}$	BHA	0.77 ± 0.15	0.45 ± 0.05	0.89 ± 0.10	0.90 ± 0.15	0.37 ± 0.05	2.72 ± 0.32	0.52 ± 0.06
		Levels of mRNA encoding ...						
Sex and genotype	Diet	Gstm4	Gstm5	Gstm6	Gstp1	Gstp2	GCLC	GCLM
Male, Nrf2$^{+/+}$	Control	1.00 ± 0.21	1.00 ± 0.11	1.00 ± 0.10	1.00 ± 0.01	1.00 ± 0.09	1.00 ± 0.04	1.00 ± 0.14
Male, Nrf2$^{-/-}$	Control	0.10 ± 0.01	0.76 ± 0.08	0.33 ± 0.05	0.85 ± 0.10	0.86 ± 0.17	0.24 ± 0.05	0.60 ± 0.07
Male, Nrf2$^{+/+}$	BHA	2.32 ± 0.43	0.79 ± 0.02	1.58 ± 0.09	1.65 ± 0.10	2.56 ± 0.37	1.01 ± 0.17	0.71 ± 0.12
Male, Nrf2$^{-/-}$	BHA	0.95 ± 0.14	1.54 ± 0.16	0.64 ± 0.05	1.16 ± 0.17	2.10 ± 0.24	0.15 ± 0.03	0.38 ± 0.10
Female, Nrf2$^{+/+}$	Control	1.00 ± 0.16	1.00 ± 0.17	1.00 ± 0.12	1.00 ± 0.12	1.00 ± 0.16	1.00 ± 0.22	1.00 ± 0.16
Female, Nrf2$^{-/-}$	Control	0.45 ± 0.08	1.03 ± 0.15	0.54 ± 0.05	0.21 ± 0.02	0.81 ± 0.07	0.41 ± 0.03	0.78 ± 0.14
Female, Nrf2$^{+/+}$	BHA	8.63 ± 0.83	1.75 ± 0.28	3.36 ± 0.28	3.47 ± 0.38	3.97 ± 0.42	1.09 ± 0.18	1.53 ± 0.40
Female, Nrf2$^{-/-}$	BHA	0.91 ± 0.12	1.13 ± 0.13	0.90 ± 0.11	0.43 ± 0.07	1.18 ± 0.17	0.12 ± 0.03	0.88 ± 0.09

phenolic antioxidant increased Gstm1 in male and female mutant mice only approx. 2.5-fold over the constitutive levels observed in Nrf2 KO mice.

The HPLC method allowed measurement of Gstm2 in mouse liver, despite the fact it is quantitatively a relatively minor transferase subunit. Table 4 shows that the constitutive level of this subunit is reduced in the absence of Nrf2. Furthermore, dietary BHA affected a > 20-fold increase in the hepatic content of Gstm2, and this induction was lost in the KO animals. The Gstm4 subunit was not abundant, and its constitutive levels could not be quantified with accuracy. Nevertheless, it was clearly inducible by BHA in WT mice, but not *Nrf2*$^{-/-}$ mice.

The expression of class Pi GST in mouse liver is sexually dimorphic, and this is influenced by Nrf2. Livers of female control WT mice contain only approx. 25% of the amount of Gstp1/2 that is found in male control WT mice (Table 4). By comparison with *Nrf2*$^{+/+}$ mice, the content of Gstp1/2 is unchanged in the livers of male mutant mice fed on a control diet. However, in the livers of female *Nrf2*$^{-/-}$ mice the amount of Gstp1/2 is reduced below that observed in female *Nrf2*$^{+/+}$ mice. As a consequence, the level of Gstp1/2 in livers of female mutant mice is only approx. 10% of that in the livers of male mice. BHA induces hepatic class Pi GST approx. 2-fold and 4-fold, respectively, in male and female WT mice. In both male and female *Nrf2*$^{-/-}$mice, induction of Gstp1/2 by BHA is abolished.

Nrf2 regulates mRNA levels for GST and GCL

TaqMan® real-time PCR assays were established to allow the effect of loss of Nrf2 on mRNAs for a range of GSH-dependent enzymes to be quantified. In the livers of male and/or female Nrf2 mutant mice, the constitutive levels of mRNA for Gsta1, Gsta2, Gstm1, Gstm3 and Gstm4 were reduced to between 3% and 20% of that in WT mice (Table 5). In addition, the levels of mRNA encoding Gsta3, Gsta4, Gstm2, Gstm6, Gstp1 and GCLC in the livers of mutant male and/or female mice fed on a control diet were reduced to between 30% and 60% of that in WT mice.

In addition to the PCR analyses described above, TaqMan® assays have been established for Nrf1, Nrf2, MafG, MafK and Keap1. It has been found that the mRNAs for Nrf1, MafG, MafK and Keap1 did not differ significantly in the livers of WT and KO mice fed on a control diet (Q. Jiang, C. R. Elcombe and J. D. Hayes, unpublished work). This is an important result, because it indicates that a general depression of transcription does not occur in the *Nrf2*$^{-/-}$ mice.

In *Nrf2*$^{+/+}$ mice, BHA affected a large induction of the mRNA encoding Gsta1 and Gstm3, with less marked induction in message for Gsta2, Gstm1 and Gstm2. More modest increases in mRNA encoding Gstm4, Gstp1 and Gstp2 were also observed. It was noted that many of these genes were more inducible in female WT mice than in male mice. This was particularly obvious with Gsta1, Gstm1, Gstm2, Gstm3, Gstm4 and Gstp1. A number of mRNAs examined, such as Gsta3 and Gstm5, appeared relatively unaffected by BHA.

Induction of gene expression by BHA in *Nrf2*$^{-/-}$ mice was variable, and could not be predicted by the response in WT mice. When allowance is made for the low constitutive expression, the mRNA species encoding Gsta1, Gsta2, Gstm1 and Gstm2 were induced by BHA in KO mice, although the relative amount of induction caused by BHA was variable. With Gstp1 and Gstp2, induction by BHA was abolished in the KO mice. Interestingly, the continuous feeding of BHA for 14 days suppressed expression of GCLC in *Nrf2*$^{-/-}$ mice.

DISCUSSION

The objective of this paper was to determine the impact disruption of *Nrf2* has on expression of GST and GCL enzymes. Initially, the cDNA for Gstm4 was cloned in order to be certain that the class Mu transferases were defined unambiguously: Gstm1, Gstm2 and Gstm3 have been described in [24,25]; Gstm4, originally called Yb_5 [22], is defined in Figure 2 of this paper; Gstm5 and Gstm6 have been reported in [26] and [28] respectively. Subsequently, in this study, TaqMan® assays were developed for all class Mu transferases and other GSTs, as well as GCLC and GCLM, to allow the expression of these antioxidant genes to be monitored.

The most striking observation of the present study is that constitutive hepatic expression of Gsta1, Gsta2, Gstm1, Gstm3, Gstm4 and GCLC is markedly reduced in *Nrf2* homozygous null mice. It is not widely appreciated that Nrf2 regulates both constitutive and inducible expression of GSH-dependent enzymes *in vivo*. Most importantly, our TaqMan® data reveal that Nrf2 influences the expression of a substantial battery of genes, including class Alpha, class Mu and class Pi GST.

Reduced constitutive expression of GSH-dependent enzymes in Nrf2 KO mice and increased sensitivity to xenobiotics

Class Alpha Gsta1 and Gsta2 subunits are both present in the livers of *Nrf2* mutant mice fed on a control diet at $< 20\%$ of the levels observed in WT mice. The Gsta1-2 heterodimer (also called GST 9.5) has been isolated from mouse forestomach [35]. It possesses at least 10-fold higher catalytic efficiency than the other transferases towards 7β,8α-dihydroxy-9α,10α-oxy-7,8,9,10-tetrahydrobenzo[*a*]pyrene, the metabolite of BaP that represents the ultimate carcinogen [36]. Gsta1-2 also has high activity towards all the stereoisomers of *trans*-3,4-dihydroxy-1,2-oxy-1,2,3,4-tetrahydrobenzo[*c*]phenanthrene [37]. It is predicted that organs of $Nrf2^{-/-}$ mice that express Gsta1/2 subunits at a reduced level will be more sensitive to polycyclic aromatic hydrocarbons than WT mice. Real-time PCR has shown that the mRNAs for Gsta1 and Gsta2 are reduced in the stomach of $Nrf2^{-/-}$ mice to approx. 40% and 10%, respectively, of the level in the stomach of WT mice. This result may explain the observation that the KO mice develop more forestomach tumours than do WT mice when treated with BaP [18]. The fact that the lungs of mutant mice are more sensitive to the genotoxic effects of diesel fumes [17] might also be attributed to the relative lack of class Alpha transferases in such animals. Specifically, TaqMan® assays have shown that the pulmonary level of mRNA for Gsta2 in the KO mouse is reduced to approx. 60% of that found in the lung of WT mice (Q. Jiang, C. R. Elcombe and J. D. Hayes, unpublished work).

Mice are intrinsically resistant to aflatoxin B_1 hepatocarcinogenesis. This is attributed to the constitutive expression in the liver of Gsta3-3, a transferase with high activity towards aflatoxin B_1-8,9-epoxide [38–40]. Table 4 shows that Gsta3 subunit levels in the liver of male $Nrf2^{-/-}$ fed on either a control or a BHA-containing diet were approx. 40% of that in WT mice. Kwak et al. [41] reported that male Nrf2-null mice accumulate 2.7-fold more aflatoxin B_1–DNA adducts following exposure to the mycotoxin than do WT mice. Collectively, these data are consistent with the hypothesis that Gsta3-3 represents a major determinant of resistance to this hepatocarcinogen.

Constitutive expression of a number of class Mu transferases was found to be dependent on Nrf2. The HPLC method indicated that the livers of $Nrf2^{-/-}$ mice contain significantly lower amounts of the Gstm1 and Gstm2 subunits than do WT mice. Similarly, the levels of mRNA species for class Mu GST in the livers of Nrf2 KO mice was reduced to 10–50% of the amount in WT mice. The physiological consequences of the reduced levels of class Mu transferases is difficult to predict, since relatively little is known about the catalytic properties of class Mu GST in the mouse. The conjugation of a number of carcinogens, including BaP-4,5-epoxide and 4-nitroquinoline 1-oxide, with GSH is catalysed *in vitro* by Gstm1-1 [23], and it is possible that Nrf2 KO mice will be sensitive to these chemicals. Clearly, experiments are required to characterize the catalytic properties of this family of enzymes.

Hepatic expression of GCLC is diminished in Nrf2-nulled mice, and this will compromise their ability to synthesize GSH in response to oxidative stress. It has been proposed that the sensitivity of the mutant mice to acetaminophen hepatotoxicity is due to an impaired ability to regenerate GSH following depletion by *N*-acetyl-*p*-benzoquinone-imine, the reactive metabolite of acetaminophen [13,14]. It is apparent that other compounds that are conjugated with GSH before biliary excretion, and are eliminated ultimately from the body as mercapturic acids, may also be toxic for similar reasons.

Mechanism of induction of the *Gsta1* gene by BHA

A large number of TaqMan® real-time PCR assays have been developed that allow measurement of individual mRNA species in mouse tissues. By means of these assays, it has been shown for the first time that class Alpha *Gsta1* is highly inducible *in vivo* by BHA. Between nt -750 and -715 of *Gsta1*, a direct repeat-type of ARE, 5′-TTGGAAATGACATTGCTAATGGTGACA-AAGCAACTT-3′ (with the 'core' ARE sequences underlined), has been identified [21]. It is reasonable to assume that this enhancer is responsible for the marked transcriptional activation of *Gsta1* by BHA in WT mice.

Mechanism of induction of class Mu and class Pi GST genes by BHA

In the present study, we have provided evidence that Nrf2 regulates the class Mu Gstm1 subunit in mouse liver. Approximately 0.6 kb flanking *Gstm1* has been cloned, and because this region does not contain a perfect ARE consensus sequence, it cannot be stated with certainty why expression of the gene is reduced in Nrf2 KO mice. An imperfect ARE sequence exists (5′-CTGACAGAGTT-3′) between nt -533 and -523 that can form a 15 bp palindrome (5′-CTGTCAGACTGACAG-3′) centred around nt -534 (underlined) [42]. It is not known whether this motif in *Gstm1* can act as an enhancer, but it does invite comparison with the palindromic-type of ARE in the 5′-flanking region of the rat NAD(P)H:quinone oxidoreductase 1 gene [43] that represents a high-affinity binding site for Nrf2 [44].

The TaqMan® data showed that *Gstm3* is highly inducible by BHA, a finding that confirms previous Northern blotting experiments [42,45]. However, a perfect ARE has not been identified in the promoter of this gene. To date, about 0.9 kb of the 5′-flanking region of *Gstm3* has been cloned, and the imperfect ARE sequence 5′-CTGACCTCGAA-3′ can be identified, in reverse orientation, between nucleotides -653 and -643 [42]. Mutation analysis of the core ARE in rat *GSTA2* has shown that a C → A transversion of the 3′ cytosine within the *cis*-element causes loss of inducibility, but not basal expression [3]. It therefore seems improbable that this putative enhancer is responsible for